

# **Improved Mechanical and Thermal Properties of Poly(hydroxyalkanoate) Resins through Polymer Blending and Bio-based Plasticizers**

by

**Hicham Alayan**

A thesis submitted to McGill University in partial fulfillment of the requirements of the  
degree of Master of Engineering



December 2017  
Department of Chemical Engineering  
McGill University, Montréal, Québec, Canada

© Hicham Alayan (2017)

*Hier encore, j'avais vingt ans, je gaspillais le temps  
En croyant l'arrêter  
Et pour le retenir, même le devancer  
Je n'ai fait que courir et me suis essoufflé*

*– Charles Aznavour*

*Dedicated to my two most precious:  
Amin and Wafaa.*

## ABSTRACT

Poly(hydroxyalkanoates) are biodegradable, biocompatible and naturally-occurring polymers produced by microbial fermentation under nutrient-deficient conditions. Commercial applications of such polymers are limited by their weak mechanical properties and thermal sensitivity. Poly(3-hydroxybutyrate-co-3-hydroxyvalerate) (PHBV), poly(3-hydroxybutyrate) (c-PHB) and poly(3-hydroxybutyrate-co-4-hydroxybutyrate) (a-PHB) are all different types of poly(hydroxyalkanoates). In this study, the mechanical and thermal properties of polymer blends composed of PHBV, c-PHB, a-PHB and selected bio-based plasticizers: epoxidized soybean oil (ESO), stearic acid (SA) and diheptyl succinate (DHPS) are examined. The effects of crosslinking using dicumyl peroxide (DCP) and filling with calcium carbonate ( $\text{CaCO}_3$ ) are also studied. Extrusion was used to prepare the blends, and hot-press molding was used to produce the tensile test bars. The mechanical and thermal properties of the blends were then characterized using tensile testing and differential scanning calorimetry, and compared with those of the polymers. Experiments revealed synergistic effects between c-PHB and a-PHB, in which the melt blending of 10 – 30 wt% a-PHB with c-PHB resulted in blends with higher toughness compared to both, c-PHB and a-PHB. Moreover, ESO/SA and DHPS were both effective in plasticizing a-PHB, but exhibited opposing effects on its flexibility. Melt blending of 5 parts per hundred rubber (PHR) ESO and 1 PHR SA to a-PHB increased its elongation at break from 65% to 92% and increased its elastic modulus from 7 MPa to 13 MPa compared to neat a-PHB, while melt blending of 40 PHR DHPS with a-PHB increased its elongation at break from 65% to 85% and reduced its tensile modulus from 7 MPa to 3 MPa. Consistent toughening effects were observed with the addition of similar ESO/SA loadings to blends composed of 20 wt% PHBV and 80 wt% a-PHB, while consistent softening effects were observed with the addition of a similar DHPS loadings to PHBV or to polymer blends already plasticized with ESO/SA. Finally, melt blending of 10 PHR  $\text{CaCO}_3$  and 1 PHR DCP with blends composed of 20 wt% PHBV and 80 wt% a-PHB resulted in blends with higher tensile strength, lower elongation at break and lower flexibility. The findings showed the potential to selectively tune the mechanical and thermal properties of poly(hydroxyalkanoates) using biodegradable bio-based components and to develop novel bioplastic products using poly(hydroxyalkanoates).



## RÉSUMÉ

Les poly(hydroxy alcanoate)s sont des polymères biodégradables, biocompatibles et des produits naturels obtenus par fermentation microbienne dans des conditions d'appauvrissement des nutriments. Les applications commerciales de tels polymères sont limitées par leurs faibles propriétés mécaniques et leur sensibilité thermique. Les polymères poly(3-hydroxybutyrate-co-3-hydroxyvalérate) (PHBV), poly(3-hydroxybutyrate) (c-PHB) et poly(3-hydroxybutyrate-co-4-hydroxybutyrate) (a-PHB) sont tous des différents types de poly(hydroxyalcanoate)s. Dans cette étude, nous examinons les propriétés mécaniques et thermiques de mélanges de polymères composés de PHBV, c-PHB, a-PHB et de plastifiants naturels particuliers: l'huile de soja époxydée (ESO), l'acide stéarique (SA) et le diheptyl succinate (DHPS). Nous examinons également l'effet de la réticulation en utilisant le peroxyde de dicumyle (DCP) et le remplissage avec du carbonate de calcium ( $\text{CaCO}_3$ ). Nous avons utilisé l'extrusion pour préparer les mélanges et le moulage à chaud pour produire les barres de traction. Nous avons ensuite caractérisé les propriétés mécaniques et thermiques des mélanges à l'aide de tests de traction et de calorimétrie à balayage différentiel, et nous les avons également comparés à ceux des polymères. Nos expériences ont révélé des effets synergiques entre le c-PHB et le a-PHB. En effet, le mélange en fusion de 10-30% en poids de a-PHB avec du c-PHB conduisait à des mélanges montrant une ténacité plus élevée que les c-PHB et a-PHB indépendamment. En outre, ESO / SA et DHPS étaient tous deux efficaces pour la plastification du a-PHB, mais présentaient des effets opposés sur sa flexibilité. Le mélange à l'état fondu de 5 parties par 100 de caoutchouc (PHR) ESO et 1 PHR de SA à a-PHB a augmenté son allongement à la rupture de 65% à 92% et a augmenté son module élastique de 7 MPa à 13 MPa comparé au a-PHB pur, tandis que le mélange à l'état fondu de 40 PHR DHPS avec a-PHB a augmenté son allongement à la rupture de 65% à 85%, et réduit son module de traction de 7 MPa à 3 MPa. Des effets de trempe uniformes ont été observés avec l'ajout de charges ESO / SA similaires à des mélanges composés de 20% en poids de PHBV et de 80% en poids de a-PHB, tandis que des effets de ramollissement constants ont été observés avec des charges DHPS similaires au PHBV ou aux mélanges de polymères déjà plastifiés avec ESO / SA. Enfin, le mélange à l'état fondu de 10 PHR de  $\text{CaCO}_3$  et 1 PHR de DCP avec des mélanges composés de 20% en poids de PHBV et de 80% en poids de a-PHB a conduit à des mélanges ayant une résistance à la traction, un allongement à la rupture et une flexibilité inférieurs. Nos résultats rendent compte de la possibilité d'ajuster les propriétés mécaniques et thermiques des poly(hydroxy alcanoate)s en utilisant des composants naturels biodégradables, et de développer de nouveaux produits bioplastiques en utilisant des poly(hydroxy alcanoate)s.

## ACKNOWLEDGMENTS

I would like to first express my deep gratitude to my supervisors Dr. Milan Maric, Dr. Richard Leask and Dr. Jim Nicell for their constant guidance and support during my research, their trust and their patience. Dr. Jim Nicell was exceptionally generous with his invaluable insights on some of my personal initiatives, mentorship and inspiration.

This project was made possible by funding from the Natural Sciences and Engineering Research Council of Canada (NSERC) through the Engage Grant and the CREATE in Green Chemistry program.

I would like to recognize the efforts of Petr Fiurasek (CSACS) in training me on differential scanning calorimetry and thermogravimetric analysis, and Dr. Robin Stein (Department of Chemistry) in training me on nuclear magnetic resonance spectroscopy.

I am grateful to my colleagues in the 'Green Plasticizers' research group: Marlon Bustos, Roya Jamarani, Basant Elsiwi, Dr. Mazeyar Gashti, Dr. Omar Garcia-Valdez and Adrien Métafiot for their feedback on my presentations, their scientific advice and friendship. I would like to also mention my office-mates: Faezeh Hajiali, Kelly Stark and Maryam Eslami for their joyful company and friendship.

Further recognition goes to my mentors: Dr. Taleb Ibrahim, Helen Bigland, Haroun Chetibi, Halim Hardan and Sami Hassouneh whom I am always grateful for. Their support throughout my professional journey, their invaluable advices and their fruitful friendship have helped me realize my genuine career interests and develop my skills and abilities.

I would like to thank my wonderful friends who I met in Montréal: Haider, Dr. Abla, Mohab, Mo-Sakr, Jalal, Kaddoura, Yassine (Mr. SuperDad), Musaab, Hussam, Francis (cyber star), Omar-Daniel (my big brother), Tarek, Sonia, Ihsan, Firas, Christina, Mo-Salah, Aloïs, Mahmoud(s), Aqeel and Diraki. They made my past two years a wonderful and joyful journey and I am evermore grateful for their friendship and support.

During the last two years, I had the chance to enjoy my favorite sport and develop friendships for which I am thankful for. I would like to thank Coach Ryan Brant from the McGill Volleyball Team for his devotion and persistence, assistant coaches, administration and my fellow team members: Damian, Scott, Andreas, Andrew, Tim, Raed, Josh, Will, Zain, Antoine, Thomas, Omar, Makram, Jack and Aleksandar whom I enjoyed the most memorable challenges and adventures with. Recently, I joined Everton Volleyball Club in Montréal to find myself between a group of enthusiastic high-caliber athletes and an inspirational coach whom I am thankful for. Namely, Coach Sergiu Ilies, Massi, Fernando, Matei, Joel, Jérémie, Pierre, Joachim, François, Martin, Gustavo, Mehdi, Amin and Manu. I am enormously grateful for their delightful friendship that goes far beyond the court and for their continuous support after my ankle fracture to come back even stronger than before.

I would like to also mention my friends back in Dubai who were always by my side in good times and bad times, and whom I missed a lot during my last two years in Montréal. Special thanks go to Moti, Rahmani, Marwan, Suweidi, Youssef, Ali, Pouya, Raha, Salah, Jardali, Ammar, Mounir, Aziz, Ghaddar, Ramazan, Nodar, Boris and Caroline.

Finally, and most importantly, I would like to thank my cherished parents, Amin and Wafaa, my beloved sister, Bushra, and my dear brother, Bassam, for their never-ending love, encouragement and support. They are my pride, my joy and my everyday inspiration. They are absolutely my everything. I am also grateful to: my grandfathers, Abu Issam (RIP) and Abu Moeen; my grandmothers, Amna and Mona; and my Uncles and Aunts: Mo, Ayad, Hanan, Issam (RIP), Mahmoud, Abdallah, Walid, Hayat, Youssef and Adnan who were, are, and will always be there for me no matter how much distances set us apart.

## **CONTRIBUTION OF AUTHORS**

Hicham Alayan is the primary author of this document and the main contributor to the design of experiments, data collection, data analysis, data interpretation and drafting of all written work. Prior to publishing, this document was reviewed and edited by Dr. Milan Maric, Dr. Richard L. Leask and Dr. Jim A. Nicell. Samples of the novel 'green' plasticizer that were utilized in this study were generously provided by Basant Elsiwi and Dr. Omar Garcia-Valdez.

# TABLE OF CONTENTS

Abstract	I
Résumé	II
Acknowledgments	III
Contribution of Authors	V
Table of Contents	VI
List of Figures	VIII
List of Tables	IX
Abbreviations	X
Nomenclature	XI
 1. INTRODUCTION	 1
 2. OBJECTIVES	 4
 3. LITERATURE REVIEW	 5
3.1 POLY(HYDROXYALKANOATES)	5
3.1.1 Background	5
3.1.2 Poly(3-hydroxybutyrate)	7
3.1.3 Poly(3-hydroxybutyrate-co-3-hydroxyvalerate)	7
3.1.4 Poly(3-hydroxybutyrate-co-4-hydroxybutyrate)	8
3.2 COMPOUNDING	9
3.2.1 Polymer Blending	9
3.2.2 Plasticizing	10
3.2.3 Fillers	12
3.2.4 Crosslinking	13
 4. MATERIALS AND EXPERIMENTAL PROCEDURES	 16
4.1 MATERIALS	16
4.2 POLYMER CHARACTERIZATION	17
4.2.1 NMR Spectroscopy	17
4.2.2 Thermogravimetric Analysis	17
4.2.3 Differential Scanning Calorimetry	17

4.3 BLENDS PREPARATION	18
4.3.1 Extrusion	18
4.3.2 Hot-Press Molding	20
4.3.3 Tensile Strength Testing	22
4.4 REPLICATES	24
5. RESULTS	26
5.1 <sup>1</sup> H NMR COMPOSITION ANALYSIS	26
5.2 THERMOGRAVIMETRIC ANALYSIS	27
5.3 NEAT POLYMERS AND NEAT POLYMER BLENDS	28
5.4 PLASTICIZING WITH ESO AND SA	30
5.5 PLASTICIZING WITH DHPS	33
5.6 FILLING WITH CaCO <sub>3</sub> AND CROSSLINKING USING DCP	36
6. DISCUSSION	38
6.1 NEAT POLYMERS AND NEAT POLYMER BLENDS	39
6.2 PLASTICIZING WITH ESO/SA	41
6.3 PLASTICIZING WITH DHPS	44
6.4 CROSSLINKING USING DCP AND FILLING WITH CaCO <sub>3</sub>	46
7. CONCLUSION AND FUTURE WORK	49
7.1 CONCLUSION	49
7.2 FUTURE WORK	50
8. ORIGINAL CONTRIBUTIONS	52
REFERENCES	54
APPENDIX – A	66

## LIST OF FIGURES

Figure 3.1 – Molecular structures of: (a) c-PHB; (b) PHBV; (c) a-PHB.	6
Figure 3.2 – Crosslinking of PHBV using dicumyl peroxide (DCP) [62].	14
Figure 4.1 – Conical intermeshing twin-screw extruder.	18
Figure 4.2 – Collection of extrudate: (a) extrudate coming out from extruder; (b) chopped extrudate to be utilized in hot-press molding.	20
Figure 4.3 – Hot-press molding machine (Carver Manual Hydraulic Press with Watlow Temperature Controllers, Model #3856, Carver Inc.).	21
Figure 4.4 – Preparation of tensile test bars: (a) steel molds filled with chopped extrudate; (b) collected tensile bars after hot-press molding.	21
Figure 4.5 – Dimensions of tensile testing bars in accordance to ASTM D-638 (2003) [112].	22
Figure 4.6 – Tensile strength tester (Shimadzu EZ Test).	23
Figure 5.1 – NMR spectrum of PHBV sample.	26
Figure 5.2 – TGA plots of PHBV sample.	27
Figure 5.3 – Typical stress-strain curves of neat polymers and neat polymer blends: (a) c-PHB, c-PHB/a-PHB (90:10), c-PHB/a-PHB (80:20), c-PHB/a-PHB (70:30), PHBV; (b) c-PHB/a-PHB (20:80), PHBV/a-PHB (20:80), a-PHB.	28
Figure 5.4 – DSC curves of neat polymers and neat polymer blends: (a) second heating cycle; (b) cooling cycle.	29
Figure 5.5 – Tensile effects of ESO and SA on blends: (a) elongation at break (%); (b) tensile strength (MPa); (c) elastic modulus (MPa).	31
Figure 5.6 – DSC curves of blends with ESO and SA: (a) second heating cycle; (b) cooling cycle.	32
Figure 5.7 – Tensile effects of DHPS on blends: (a) elongation at break (%); (b) tensile strength (MPa); (c) elastic modulus (MPa).	34
Figure 5.8 – DSC curves of blend plasticized with DHPS: (a) second heating cycle; (b) cooling cycle.	35
Figure 5.9 – Tensile effects of CaCO <sub>3</sub> /DCP on typical stress-strain curve.	36
Figure 5.10 – DSC curves of blend with CaCO <sub>3</sub> /DCP: (a) second heating cycle; (b) cooling cycle.	37

## LIST OF TABLES

Table 4.1 – List of utilized additives.	16
Table 4.2 – Extrusion operating conditions.	19
Table 5.1 – Mechanical properties of neat polymers and neat polymer blends.	29
Table 5.2 – Thermal properties of neat polymers and neat polymer blends.	30
Table 5.3 – Mechanical properties of blends with ESO and SA.	32
Table 5.4 – Thermal properties of blends with ESO and SA.	32
Table 5.5 – Mechanical properties of blends with DHPS.	35
Table 5.6 – Thermal properties of blends with DHPS.	35
Table 5.7 – Mechanical properties of blends with DCP/CaCO <sub>3</sub> .	36
Table 5.8 – Thermal properties of blends with DCP/CaCO <sub>3</sub> .	37
Table 6.1 – Solubility parameters of polymers and ESO/SA including: overall solubility parameter ( $\delta$ ), dispersion component ( $\delta_d$ ), polar component ( $\delta_p$ ) and hydrogen bonding component ( $\delta_h$ ) of the polymers, ESO and SA	43
Table 6.2 – Solubility parameters of polymers, ESO/SA and DHPS including: overall solubility parameter ( $\delta$ ), dispersion component ( $\delta_d$ ), polar component ( $\delta_p$ ) and hydrogen bonding component ( $\delta_h$ ) of the polymers, ESO/SA and DHPS.	46



## ABBREVIATIONS

PHA	poly(hydroxyalkanoate)
PHB	poly(hydroxybutyrate)
c-PHB	crystalline poly(3-hydroxybutyrate)
a-PHB	amorphous poly(3-hydroxybutyrate-co-4-hydroxybutyrate)
PHBV	poly(3-hydroxybutyrate-co-3-hydroxyvalerate)
HB	hydroxybutyrate
HV	hydroxyvalerate
PP	polypropylene
PET	polyethylene
PCL	poly( $\epsilon$ -caprolactone)
PBS	poly(butylene succinate)
SO	soybean oil
ESO	epoxidized soybean oil
SA	stearic acid
PVA	polyvinyl alcohol
PLA	poly(lactic acid)
TEC	triethyl citrate
DHPS	diheptyl succinate
PHR	parts per hundred rubber
DEHP	di(2-ethylhexyl) phthalate
DCP	dicumyl peroxide
CaCO <sub>3</sub>	calcium carbonate
GHG	greenhouse gases
NMR	nuclear magnetic resonance
TGA	thermogravimetric analysis
DSC	differential scanning calorimetry
GPC	gel permeation chromatography
PPO	poly(2,6-dimethyl-1,4-phenylene oxide)
PS	polystyrene

## NOMENCLATURE

$M_t$	Metric tons
$T_g$	Glass transition temperature
$T_m$	Melting temperature
$T_c$	Crystallization temperature
$\Delta H_m$	Latent heat of melting
$\Delta H_c$	Latent heat of crystallization
$L_o$	Initial distance between metal grips of the tensile tester
$L$	Distance between metal grips recorded by tensile tester
$F$	Tensile force applied by tensile tester
$T_o$	Initial thickness of the center region of the tensile test bar
$W_o$	Initial width of the center region of the tensile test bar
$\delta$	Overall solubility parameter
$\delta_d$	Dispersion component of the solubility parameter
$\delta_p$	Polar component of the solubility parameter
$\delta_h$	Hydrogen bonding component of the solubility parameter

# 1. INTRODUCTION

The low cost and durability of plastics led to their wide utilization in products such as packaging materials, building materials, agricultural materials, commodities and hygiene products [1,2]. The same durability characteristics permit plastics to resist biodegradation and accumulate in different forms in the environment as near-permanent contaminants. The amount of plastics manufactured from 1950 to 2015 is estimated to be 7,800 million metric tons (Mt), with half of that amount produced in the past 13 years only [3]. More than 79% of the plastic wastes generated since 2015 were deposited in landfills or dumped into oceans, accounting to more than 5,000 Mt of plastic wastes [3]. It is estimated that 4 to 12 Mt of plastic wastes were disposed in the marine environment in 2010 alone [4]. The production growth of plastics has surpassed most anthropogenic materials and has drastically exceeded our planet's capacity to absorb such wastes [3].

In response to the need for preservation of the environment, a global awareness grew years ago about the negative impacts of plastics, and extensive ongoing efforts were directed towards plastics recycling and incineration technologies. However, although recycling delays the disposal of plastic wastes through reprocessing into secondary materials and offsets a portion of the needs to produce virgin plastics from limited resources, it does not prevent their final disposal [3]. Additionally, reprocessed plastics often have a lower technical and economic value than virgin plastics due to their contamination and the impurities resulting from blending of different types of polymers and additives [3]. The need for plastics with less harmful environmental impacts stimulated research in biodegradable plastics, which led to the development of polymers such as polyglycolide (PGA), polylactide (PLA), polycaprolactone (PCL), poly(butylene adipate-co-terephthalate) (PBAT) and polyvinyl alcohol (PVA).

In the late 1970's, peak oil prices accelerated research in naturally-occurring polymers, such as those produced by microorganisms and analogous to petroleum-derived polymers. Natural polymers attracted significant interest due to their complete

biodegradation, biocompatibility, piezoelectric properties and renewable nature, all of which have contributed to their wide applications in medicine, packaging and agriculture [5]. One type of natural polymers is poly(hydroxyalkanoate) (PHA). PHA is a naturally occurring polymer, which is produced using various natural feedstocks and produced under different nutrient depletion conditions [6–8]. PHA forms inside microorganisms as intracellular storage material of carbon and energy, and its composition is a function of feedstock content, bacterial strain and environmental conditions [9]. PHA-producing microorganisms are known to accumulate an amount of PHA equivalent to 30 – 80% of their cellular dry weight under conditions of limited nitrogen and abundant carbon [10].

Due to its unique characteristics, PHA is considered a viable source of plastic, with the potential to be blended with or to be directly substituted for conventional synthetic polymers. The key advantage of PHA lies in the fact that it is readily produced by microorganisms, making it an ideal biodegradable polymer. Although some biodegradable polymers like poly(lactic acid) (PLA) or poly( $\epsilon$ -caprolactone) (PCL) can have their monomers produced by microorganisms from renewable resources, an additional processing step of polymerization is required for polymer synthesis. PHA is nontoxic, resistant to ultra-violet radiation, resistant to hydrolytic degradation, water insoluble and sinks in water, which facilitates its anaerobic biodegradation in sediments [11].

Despite the desired characteristics of PHA relative to its natural synthesis and unique properties, it has not yet seen wide-spread implementation due to its weak mechanical properties and processing difficulties. Its processing difficulties are due to its low thermal stability [12,13] and its tendency to form large spherulites because of low crystallization rates [14,15]. PHA is generally brittle and suffers from a narrow processing window. Its high melting point, which is very close to its thermal degradation temperature, makes it thermally sensitive and prone to thermal degradation during processing [11]. Many studies were performed on PHA to achieve higher elongation at break, higher flexibility and lower  $T_m$  [16–21], but no practical solution yet exists. Like other polymers

produced by bacterial fermentation, another limitation of PHA is its relative high cost, which is around 3 to 4 times higher than conventional synthetic polymers [22]. A significant cost of PHA stems from processing complexities in the separation of PHA from the cellular material, which generally involves solvent extraction [11,23]. The high cost of PHA is considered potentially optimizable and, as a result, many studies aim to minimize its production costs by improving extraction processes, using byproducts or waste materials as substrates for bacterial growth, and increasing PHA production through use of mixed cultures or modified bacteria or microalgae [11].

A major challenge (and opportunity) currently facing the plastics industry nowadays is to viably produce a completely green plastic with desired mechanical and thermal properties, including high elasticity, high toughness, high flexibility and high resistance to thermal degradation. Manipulating the alkyl substituent in PHA during its synthesis is one approach to enhance its properties [21,24]. Extensive research in metabolic engineering has been directed towards exploring and developing new metabolic pathways to produce new PHA products with superior properties and wider utilization substrate range [25]. However, such studies often have uncertain outcomes and involve longer timelines than polymer processing studies, and hence, may not satisfy the urgent need for alternatives that reduce the impacts of plastics on our environment. An alternative approach is to improve the toughness and processability of PHA by blending it with other biodegradable polymers and additives to expand their applications, and eventually stimulate commercial interest and application-specific research [26–30].

## 2. OBJECTIVES

Compared to other biodegradable and biocompatible polymers, PHAs have a key advantage in being readily produced by microorganisms using renewable resources [6]. However, PHA faces significant challenges in its commercial application mainly due to its brittle structure, low elongation at break and narrow thermal processing window [11]. Therefore, the enhancement of the mechanical and thermal properties of selected PHA resins can create economically attractive opportunities for novel bioplastic applications.

This study aims to examine the mechanical and thermal properties of polymer blends composed of PHBV, c-PHB, a-PHB, and selected additives: epoxidized soybean oil (ESO), stearic acid (SA) and diheptyl succinate (DHPS) as bio-based plasticizers, dicumyl peroxide (DCP) as a cross-linker, and calcium carbonate ( $\text{CaCO}_3$ ) as a filler.

The objectives of this thesis are to:

1. Define the chemical composition and thermal degradation characterization of PHBV using Proton Nuclear Magnetic Resonance ( $^1\text{H-NMR}$ ) spectroscopy and Thermogravimetric analysis (TGA);
2. Prepare blends using twin-screw extrusion and production of the tensile test bars using hot-press molding; and
3. Quantify the mechanical and thermal properties of the following blends using tensile testing and differential scanning calorimetry (DSC):
  - PHBV, c-PHB and a-PHB neat polymers;
  - Polymer blends composed of PHBV, c-PHB and a-PHB;
  - Polymer blends plasticized with DHPS;
  - Polymer blends plasticized with ESO and SA; and
  - Polymer blends crosslinked using DCP and filled with  $\text{CaCO}_3$ .

### 3. LITERATURE REVIEW

#### 3.1 Poly(hydroxyalkanoates)

##### 3.1.1 Background

In 1925, the French microbiologist *Maurice Lemoigne* was the first to isolate and characterize PHA derivatives produced by *bacillus megaterium* [31]. It was not until several decades later that PHA received substantial interest as it was found to naturally degrade by bacteria [32,33]. Its biological synthesis, biodegradability and production from low-cost renewable feedstocks made it an ideal alternative source of bioplastic materials.

One key advantage of PHA lies in its rate and extent of biodegradation compared to petroleum-derived plastics. For example, it has been reported that its hydrolytic cleavage and complete biodegradation can be achieved within 3 to 9 months [34]. PHA biodegrades aerobically and anaerobically by many different bacteria and fungi, with end-products mostly consisting of carbon dioxide and water [34,35]. In contrast to the sudden carbon release from ancient petroleum stockpiles, carbon release from PHA biodegradation is from carbon that is already part of our current carbon cycle, and therefore, produces zero net gain or loss while reducing greenhouse gas (GHG) emissions [6].

PHA has minor or no disposal costs, and like the degradation of similar bio-wastes, the degradation of PHA enriches the soil with nutrients and increases its value [36]. PHA extraction processes generate remains equivalent to 10% of cellular dry weight, which can be utilized to recover the energy consumed by extraction [37]. Additionally, PHA and its intermediates were found in many studies to have no harmful or toxic effects on either microorganisms or animals ingesting the polymers [38,39].

PHA is the sugar-derived or lipid-derived microbial fermentation polyester product of PHA synthases [6]. It is produced by more than 75 genera of prokaryotes and archaea that are raised under nutrient-deficient conditions, in which PHAs accumulate as

intracellular energy storage reserve materials and deposit as water-insoluble inclusions in the cytoplasm [25,40]. PHA is extracted from microorganisms using solvent extraction or enzymatic treatment, in which the undesired materials are removed and PHAs are collected through filtration and centrifugation [23]. Linear polyesters of PHA, such as those shown in Figure 3.1, are made of  $10^3$  to  $10^4$  monomer subunits where the alkyl groups in most subunits are found on the C-3 carbon and range between 1 and 14 carbons in length [6].

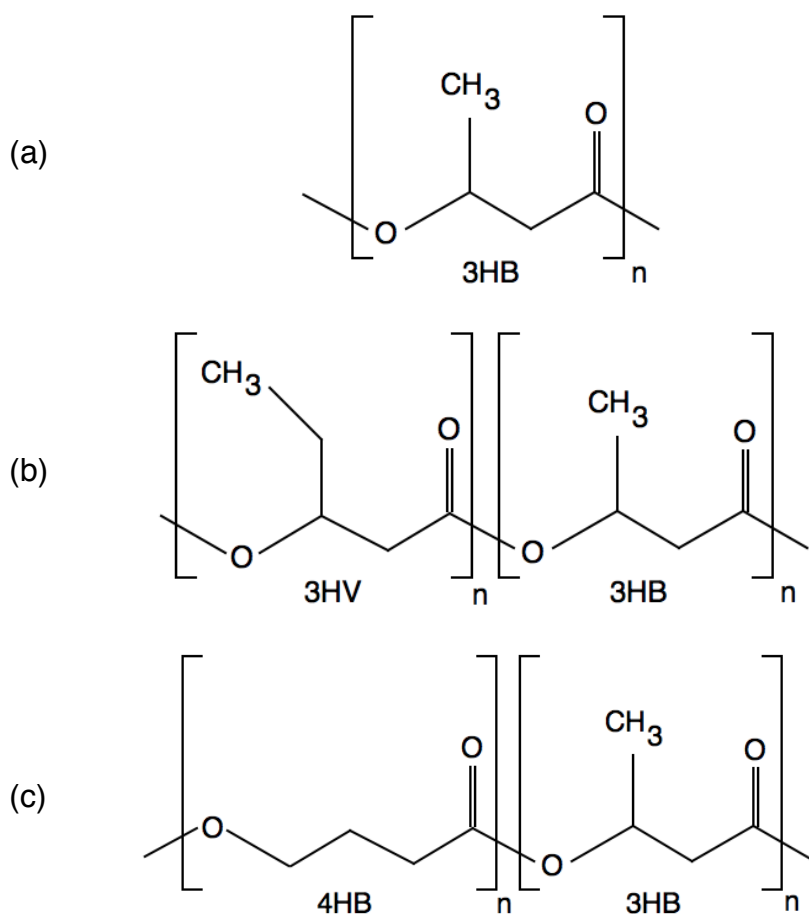


**Figure 3.1** – Molecular structures of: (a) c-PHB; (b) PHBV; (c) a-PHB.



More than 100 different PHA monomers with molecular weights ranging between 15,000 and 1,000,000 Da have been identified, with two factors contributing to such compositional variation; carbon feed sources and endogenous pathways inside the microorganism [6,7,41]. This variation in PHA compositions provides an opportunity to produce a wide range of biodegradable polymers with different physical and chemical properties. The diversity and utility of PHA arise from its potential to be assembled into heteropolymers that can be either brittle and rigid or semi-crystalline, elastic, and sticky, depending on the number of carbon atoms in its alkyl group [34].

### **3.1.2 Poly(3-hydroxybutyrate)**

One of the most commonly occurring type of PHAs is poly(3-hydroxybutyrate) (PHB). PHB behaves like a thermoplastic with an ideal versatility that is desired for any alternative to petroleum-derived polymers; it can be melt extruded, processed and applied in a similar fashion to petroleum plastics. One of the most studied types of PHB is the crystalline poly(3-hydroxybutyrate) (c-PHB), shown in Figure 3.1–(a). c-PHB is a simpler non-storage PHA with lower molecular weight, and is produced by some prokaryotes as a medium for calcium channels, DNA transport and protection of other macromolecules in the microorganism [25]. Although c-PHB is the most common form of PHB, its application is currently hampered by its narrow thermal processing window and weak mechanical properties, in which it has a melting temperature ( $T_m$ ) of 168 – 182°C, typical tensile strength of 40 MPa and elongation at break of 2 – 8% [42–44].

### **3.1.3 Poly(3-hydroxybutyrate-co-3-hydroxyvalerate)**

A second type of PHB is the copolymer of c-PHB with hydroxyvalerate (HV) monomer units, which is called poly(3-hydroxybutyrate-co-3-hydroxyvalerate) (PHBV), shown in Figure 3.1–(b). In 1983, PHBV was found to naturally occur in microorganisms upon the addition of propionic acid to the growth medium under conditions of limited nitrogen [45]. In 1990, PHBV was commercially introduced by Imperial Chemical

Industries (ICI) [46]. Its properties that are similar to those of polypropylene (PP) and polyethylene (PET) attracted significant interest as it qualified the material for a wider range of applications [47]. PHBV exhibits a highly crystalline and brittle structure that is less brittle than c-PHB, and exhibits higher flexibility and higher biodegradation rates with increasing HV content [5]. PHBV has a  $T_m$  of 144 – 172°C, a glass transition temperature ( $T_g$ ) of -5 – 20°C and a thermal degradation temperature of 180 – 200°C, all of which are lower than those of c-PHB [42,48,49]. The narrow thermal processing window between its  $T_m$  and its thermal degradation temperature presents undesired processing difficulties during melt extrusion, since friction from higher shear rates can result in elevated temperatures reaching and exceeding thermal degradation temperatures. PHBV has a tensile strength of 20 – 25 MPa and a maximum elongation at break up to 15% [49]. HV content significantly affects the thermal and mechanical properties of PHBV, in which PHBVs with higher HV content have lower crystallinity, lower  $T_m$  and  $T_g$ , and lower tensile strength [50–52]. However, most of the commercially available PHBVs have an HV content below 15 mol% [53]. PHBV is entirely biodegradable in most soil and compost conditions [54–56] and is known to have faster degradation than PHB, but processing conditions have a direct influence on their degradation rates and kinetics, both of which are highly dependent on the polymer structure and crystallinity [49]. One unique characteristic of PHBV is that it is isodimorphous; the statistical copolymer has both its monomers crystallize in form of repeating units included in the lattice of each other. This behavior has major drawbacks as it restricts a wide range of benefits from usual copolymerization. Although PHBV allows lower processing temperatures and has slightly superior mechanical and thermal properties than c-PHB, it still lacks desired properties for practical application and industrial processing, such as superior tensile properties, wider thermal processing windows and higher thermal tolerance [11].

### **3.1.4 Poly(3-hydroxybutyrate-co-4-hydroxybutyrate)**

A less common form of PHB is the copolymer of c-PHB with 4-hydroxybutyrate (4HB) monomer units, which is called amorphous poly(3-hydroxybutyrate-co-4-

hydroxybutyrate) (a-PHB), shown in Figure 3.1–(c). In 2013, a-PHB was first introduced by Metabolix under the product trademark *Mirel<sup>TM</sup> M4300*. The copolymer exhibits an amorphous behavior with a significantly higher elongation at break but lower tensile strength than both c-PHB and PHBV. A study published by Metabolix claims a significant enhancement of PLA mechanical properties upon blending with 20 wt% a-PHB, with elongation at break values reaching up to 200%, compared to PLA elongation at break of 2.5 – 6%, while maintaining a tensile strength of approximately 50 MPa [42,43,57]. The same study reported a  $T_g$  of -20°C for a-PHB [57].

## **3.2 Compounding**

Many studies examined the possibilities of blending PHA with other biodegradable polymers or additives. Key parameters that play a critical role in the development of commercially-viable PHA require them to have mechanical and thermal properties suitable for the desired application.

### **3.2.1 Polymer Blending**

Several studies have evaluated the potential of blending PHA with other biodegradable polymers. In a study that examined the effects of blending PHBV with the biodegradable poly( $\epsilon$ -caprolactone) (PCL), the blends exhibited lower crystallization rates and lower  $T_g$  values, with no significant effects on  $T_m$  compared to neat PHBV [58]. Due to the recent developments in fermented production of succinic acid and butandiol-1,4, which are the two main components of PBS, several studies investigated PHB and PHBV blends with PBS, in which the blends were found to be biodegradable under typical soil and compost conditions [59,60]. *Qiu et al* investigated the miscibility and crystallization behavior of PHBV blends with PBS and found that the blends were immiscible and exhibited lower crystallization rates with increasing PBS content, with no significant effects on the crystallization mechanisms of either PHBV or PBS [59]. The reduced rate of crystallization was attributed to the physical restriction by PBS crystals, since the

crystallization of PBS occurs at a higher temperature than that of PBHV. *Ma et al* found that the melting blending of PBS with PHB enhanced the thermal properties of PHB, increased its crystallization rate and retarded its spherulitic radial growth rate, in which PBS represented an effective nucleating agent [60]. The melt blending of PBS with PHB increased the  $T_c$  and  $T_m$  of PHB by 30°C and 10°C, respectively, with no significant effects on the  $T_m$  of PBS [60]. However, blends of PBS and PHB were incompatible and exhibited phase separation with larger particle sizes and poor interfacial adhesion [61]. Compatibilities are generally enhanced by reactive polymer blending techniques such as branching/cross-linking, grafting and formation of hydrogen bonding [62].

Since PHAs are considered ideal alternatives to petroleum-derived plastics, and blending them with other biodegradable polymers may result in phase-separated blends, it may be advantageous to blend different types of PHA with each other (as they would be expected to be miscible), together with an appropriate additive package.

### **3.2.2 Plasticizing**

Many studies examined the possibility of utilizing bio-based plasticizers to improve the mechanical and thermal properties of PHA. The term ‘bio-based’ refers to materials that are obtained from renewable resources, such as vegetable oils and starch crops, and are generally biodegradable [6]. Epoxidized soybean oil (ESO) is a vegetable oil that is widely utilized as an eco-friendly plasticizer and stabilizer for plastics in food contact materials, due to its low toxicity and low migration [63–67]. It has been utilized to plasticize polyvinyl chloride (PVC), chlorinated rubber and polyvinyl alcohol (PVA) emulsions. ESO showed significant improvement in toughness through blending modification or grafting [68–71]. It was compatible with PVC and increased its thermal stability [72]. PVC blends often contain 25 – 45 wt% ESO when added as a plasticizer, and 0.5 – 2 wt% ESO when added as a stabilizer [66,73–75]. ESO can effectively plasticize bioplastics such as PLA, improving its elongation at break and melt strength, mainly because of the adhesion of its molecules with PLA. When 9 wt% ESO was added to PLA, it improved its elongation at

break from 3.9% to 6.5% [76]. Optimum overall results were achieved when 6 wt% ESO was added to PLA, in which it increased in its elongation at break from 3.9% to 5.4%, reaching the maximum melt strength, which was 5.5 times that of pure PLA [76]. Like many other vegetable oils, ESO generally contains varying amounts of saturated fatty acids such as stearic acid (SA) and palmitic acid, which depends on plant type, weather, and geographical location of growth [77]. The unreactive saturated components of ESO such as SA and palmitic acid are known to improve the flexibility and the degree of freedom for movements of the molecular chains in the epoxy network, which eventually lead to lower  $T_g$  values [77]. Similarly, SA had direct effects in reducing the melt viscosity and acting as a normal lubricant when added to PVC in small amounts ranging between 0.5 to 1 PHR [78]. SA was also utilized as a compatibilizer to composites of c-PHB/starch plasticized with glycerol [79].

Moreover, some PVC plasticizers such as partial fatty esters, glycerols and low molecular weight citrates have exhibited plasticizing effects on biodegradable and biocompatible polymers like PLA [80–82]. In a study by *Ljunberg and Wesslen*, the addition of each of triacetin, tributyl citrate, triethyl citrate (TEC), acetyl tributyl citrate and acetyl triethyl citrate to PLA resulted in a significant improvement in elongation at break at the expense of tensile strength, a significant reduction in  $T_g$  and a homogeneous and flexible film [83]. TEC is a PVC plasticizer that showed superior plasticizing effects when added to PHBV compared to soybean oil (SO), ESO and dibutyl phthalate, in which it resulted in lower  $T_g$  values and higher elongation at break [84]. Similarly, polymers such as poly(ethylene oxide) [85,86], poly(ethylene glycol) [85] and poly(vinyl acetate) [87] have also been successful in plasticizing PLA.

Over the past decade, several bio-based monoesters and di-esters of succinic acids have been shown to be compatible with PVC, demonstrating plasticizing capabilities comparable to the common PVC plasticizer, di(2-ethylhexyl) phthalate (DEHP) [88–90]. Succinic acid plasticizers were highlighted as potential ‘greener’ alternatives to DEHP, exhibiting superior biodegradation and plasticizing effects on PVC, with a significant

influence of alkyl chain lengths of the succinic acid plasticizers on their plasticizing effectiveness [90]. In recent work by *Elsawi et al*, diheptyl succinate (DHPS) was produced from renewable feedstock and exhibited superior biodegradation and plasticizing properties compared to other succinic acid plasticizers when added to PVC at concentrations between 20 and 60 PHR [91]. DHPS was viewed as a true 'green' alternative to other PVC plasticizers due to its low toxicity, renewable nature, biodegradability and 'greener' synthesis [91]. Although no large-scale production cost estimates are yet developed, DHPS is expected to have certain economic advantages arising from its simple synthesis, high yields and high purity, with no requirements for additional purification [91].

The overall effectiveness of a plasticizer can be related to its miscibility with the polymer. In a review by *Verhoogt et al*, the effects of miscibility on the properties of blends composed of PHA and non-biodegradable thermoplastics were studied [92]. Significant drawbacks were realized as miscible blends exhibited much slower biodegradation than immiscible blends, primarily arising from the restriction of enzymatic access to the biodegradable polymer [92]. Although immiscible blends often exhibited rapid rates of biodegradation, efficient industrial production of immiscible blends is likely infeasible due to limited morphological control that restricts the ability to reproduce such blends [92]. Immiscible blends can also cause the undesired release of non-biodegradable polymers into the environment; hence, blending of PHA with biodegradable components is often recommended [92].

### **3.2.3 Fillers**

Fillers are rigid solid particulate materials (organic or inorganic) that were traditionally used to moderately increase the elastic modulus of polymers, while maintaining or reducing its tensile strength [93]. Fillers can reduce the overall cost of the material by replacing the most expensive polymer, by possibly improving the speed of molding cycles due to higher thermal conductivity, and by reducing the amount of rejected

parts resulting from warpage [93]. Frequently used fillers include montmorillonite [94], silica [93,95], aluminum oxide [96] and calcium carbonate ( $\text{CaCO}_3$ ) [97–99].

$\text{CaCO}_3$  is the most commonly used filler for thermoplastics [100] and is usually prepared by grinding the natural mineral or synthetic calcite, which is generally produced through the carbonatation of calcium hydroxide [101]. A common method to assist the dispersion of  $\text{CaCO}_3$  in the polymer matrix by diminishing the particle-particle interactions is through surface modification of  $\text{CaCO}_3$  using SA as a reagent [102]. Adsorption of SA from a toluene solution can form a monolayer on  $\text{CaCO}_3$ , resulting in a significant decrease in its surface energy [101]. Surface modification using SA can prevent the loss of mechanical performance and enhance the processability of polymers, provide means for color control and reduce long-term heat aging [93]. Several studies have shown that the addition of 5 – 40 wt%  $\text{CaCO}_3$  to c-PHB improved its elastic modulus, but at the cost of elongation at break and tensile strength [103,104]. The optimum  $\text{CaCO}_3$  dosage in a polymer blend should balance between minimum acceptable mechanical properties for a specific application and minimum overall material cost.

### 3.2.4 Crosslinking

PHBV, c-PHB and a-PHB are all linear polymers with low degradation temperatures, high crystallinity and poor melt elasticity, resulting in their poor processability [105]. One proven method to modify the properties of a polymer and their processability is crosslinking, which can be accomplished by the addition of small amounts of a peroxide in the blend. Dicumyl peroxide (DCP) is a branching or crosslinking agent that is often utilized due to its relatively high hydrogen abstraction ability. As shown in Figure 3.2, when DCP is added to PHBV at high temperatures, it forms free radicals which abstract hydrogen from tertiary  $-\text{CH}$  along the PHBV matrix, resulting in new macromolecular radicals that react with each other to form C–C covalent bonds [105].

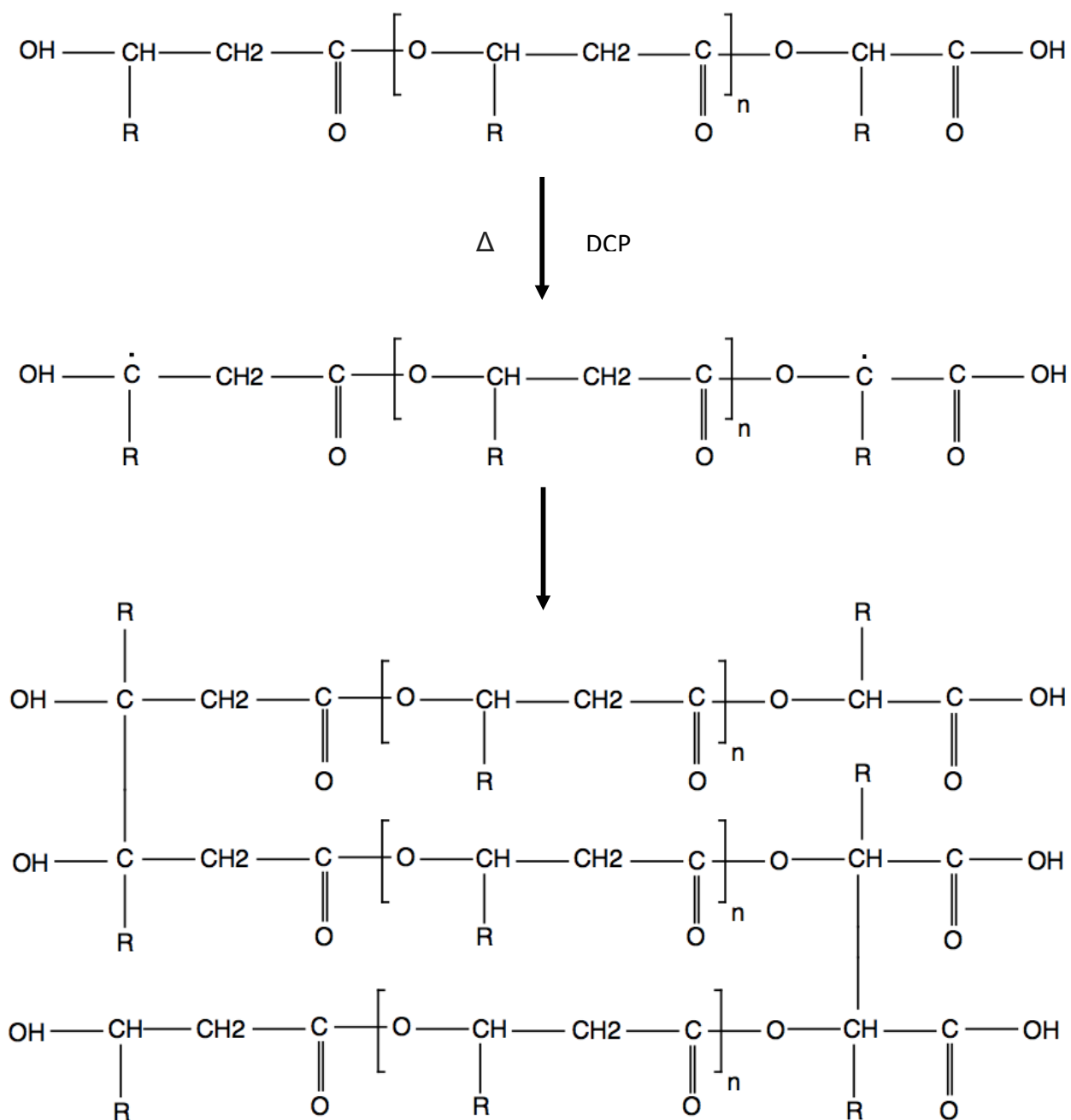


**Figure 3.2** – Crosslinking of PHBV using dicumyl peroxide (DCP) [62].



In a study by *Ma et al*, the addition of dicumyl peroxide (DCP) to a blend of PHBV and PBS resulted in reactive compatibilization of the blend during melt blending, and significantly improved its mechanical properties [61]. The DCP initiated free radical interaction between the polymer causing a reduction in the domain size of the dispersed phase and a significant interfacial adhesion. The addition of 0.5 wt% DCP and 20 wt% PBS to PHBV was found to increase the elongation at break of neat PHBV from <10% to 400% with a slight improvement in tensile strength. However, such significant improvements in elongation at break and tensile strength were not achieved with c-PHB; this was eventually attributed to the poor properties and processability of c-PHB [61]. Similar results were observed by *Wang et al* on PLA/PBS blends where, although the addition of 0.2 wt% DCP to a PLA/PBS (80:20) resulted in immiscible blends on molecular level, it resulted in a finely distributed dispersed phase in the matrix and consequently increased the elongation at break from 24% for neat PLA to more than 200% [106]. These studies show the potential DCP as a compatibilizer and its potential effects in improving the mechanical properties of PHAs.

Although DCP is often utilized in very small amounts (< 1 wt%) in polymer blends, it is important to note that DCP is synthetically produced from non-renewable resources and is not expected to biodegrade in soil [107]. Its biodegradability limitation may be of concern due to environmental waste accumulation. An ideal alternative would be one that is readily biodegradable and produced from renewable resources.

## 4. MATERIALS AND EXPERIMENTAL PROCEDURES

### 4.1 Materials

The following 3 resins were utilized in this project:

1. PHBV as a crystalline copolymer composed of HV and 3HB monomer units. The resins are in the form of < 3 mm diameter uniform pellets, with a labelled HV content of 12 mol%. This product was purchased from Sigma Aldrich (Oakville, ON, Canada).
2. c-PHB as a crystalline copolymer composed mostly of 3HB monomer units with traces of 4-HB monomer units. The resins were in the form of < 5 mm diameter flake pellets. This product was supplied by Metabolix (Woburn, MA, USA).
3. a-PHB as an amorphous copolymer composed of 3HB and 4HB monomer units. The resins are in form of < 3 mm diameter flake pellets. This product was supplied by Metabolix (Woburn, MA, USA) under the product trademark *Mirel<sup>TM</sup> M4300*.

The additives utilized in this project are shown in Table 4.1.

**Table 4.1** – List of utilized additives.

Material	Function	Supplier
ESO	Plasticizer	Chemtura (Philadelphia, PA, USA)
SA	Lubricant	Fisher Scientific (Montréal, QC, Canada)
DHPS	Plasticizer	Synthesized [91]
DCP	Cross-linker	Sigma Aldrich (Saint Louis, MO, USA)
CaCO <sub>3</sub> **	Filler	Fisher Scientific (Hampton, NH, USA)

\*Synthesized in McGill University laboratories using sustainable raw materials [91]:

1. n-heptanol (obtained from Arkema - linear seven-carbon fatty alcohol that is 100% of vegetable origin, processed from castor oil).
2. succinic acid (obtained from Reverdia - derived from a yeast-based fermentation process).

\*\*CaCO<sub>3</sub> is coated with 2 wt% SA using solvent casting method, based on study by *Jeong et al* [108].

## **4.2 Polymer Characterization**

### **4.2.1 NMR Spectroscopy**

$^1\text{H}$ -NMR spectroscopy was performed using a 300 MHz Varian Mercury NMR equipped with an SMS-100 sample changer in order to confirm the chemical structure and relative composition of HV to 3HB units in PHBV. Deuterated chloroform ( $\text{CDCl}_3$ ) was used as a solvent to prepare a 1 – 2 wt% solution of PHBV. The composition of HV expressed in mole percent of the PHBV copolymer was calculated as the area under the peak of the resonance of HV methyl unit divided by the sum of the areas under the peaks of the resonances of HV and 3HB methyl units.

### **4.2.2 Thermogravimetric Analysis**

TGA was performed using a thermogravimetric analyzer (TA Instruments Q500) to analyze the thermal degradation behavior and estimate the degradation temperature of PHBV. The analysis was performed from a temperature of 30 to 340 °C at a rate of 20 °C/min. The sample weight used was approximately 7.5 mg.

### **4.2.3 Differential Scanning Calorimetry**

DSC was performed using a temperature modulated differential scanning calorimeter (TA Instruments Q2000) to estimate  $T_g$ ,  $T_m$  and  $T_c$  of polymers and polymer blends. Thin slices weighing a total of approximately 5 – 10 mg were cut from the blend extrudate and placed in the standard DSC pan (TA Instruments, model #070221). The weight of the DSC pan with the top cover was measured using the Sartorius CP225D and then placed in the auto-sampler of the DSC. The samples were heated to 180 °C at a rate of 10 °C/min, then quenched to -45 °C at a rate of 10 °C/min, then heated again to 180 °C at a rate of 10 °C/min. The first heating cycle was used to eliminate the thermal history of the sample and measure  $T_c$ , while the second heating cycle was used to measure  $T_g$  and  $T_m$  of the sample. The 'TA Universal Analysis' software was then utilized to plot the reversible heat flow versus temperature. The  $T_g$  of each polymer blend was determined

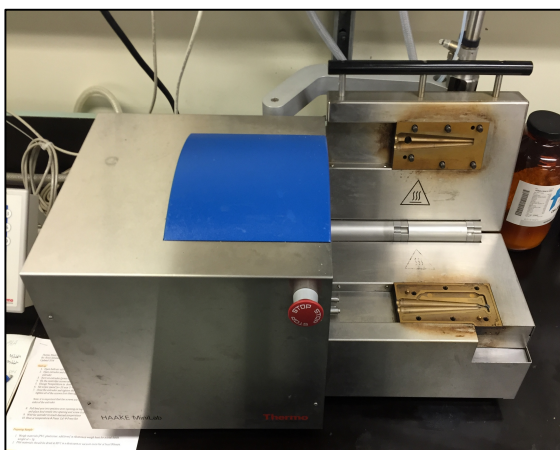
using an ASTM standard half-height technique – ASTM D-3418 (2003) - in which  $T_g$  was identified as the midpoint between the two intersection points of the tangents to the three linear regions of the reversible heat flow versus temperature graph [109].

### 4.3 Blends Preparation

Processing of polymer blends began with melt blending using extrusion, followed by collection and chopping of the extrudate, and finally hot-press molding to make tensile strength test bars. Vacuum oven drying at 60 °C was performed for 12 h prior to any thermal processing due to the hygroscopic characteristics of the polymers, in which the presence of water can result in depolymerization [27,28,60,110].

#### 4.3.1 Extrusion

Melt blending of the polymer additives was achieved using a table-top conical intermeshing twin-screw extruder (Haake Minilab, Thermo Electron Corporation) with 5/14 mm screw diameter and 109.5 mm screw length, shown in Figure 4.1. A feed size



(a)



(b)

**Figure 4.1** – Conical intermeshing twin-screw extruder: (a) twin-screw extruder (Haake Minilab, Thermo Electron Corporation); (b) conical intermeshing screws.

of 3 grams per batch was used, with a rotation speed and operating temperature that were suitably selected to ensure adequate melting and mixing at minimal temperatures. A summary of the selected extrusion operating conditions is shown in Table 4.2.

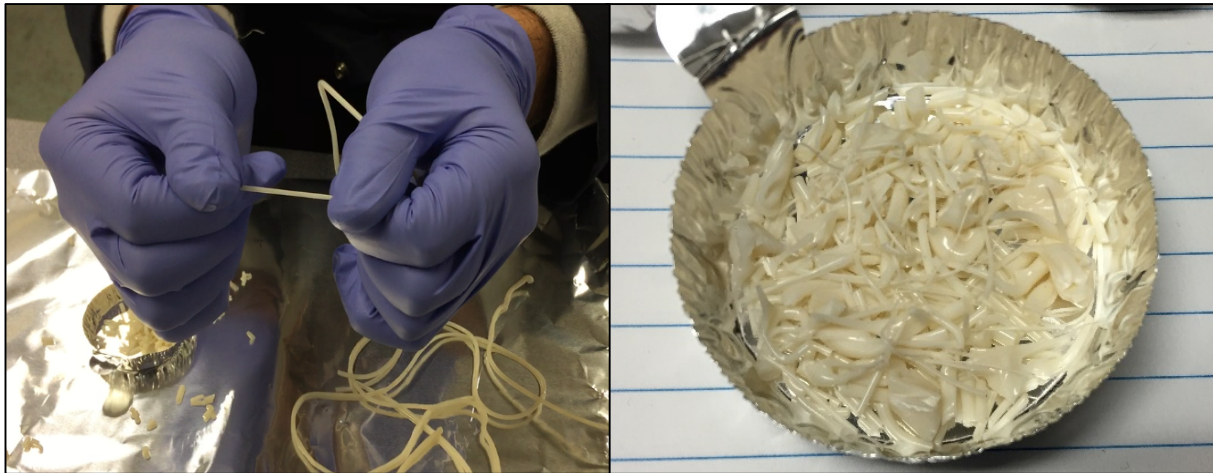
**Table 4.2 – Extrusion operating conditions.**

<b>Blend</b>	<b>Screw Speed (rpm)</b>	<b>Temperature (°C)</b>	<b>Screw Configuration</b>
PHBV	20	160	Co-rotating
a-PHB*	20	170	Co-rotating
PHBV/a-PHB (20:80)	20	170	Co-rotating
c-PHB/a-PHB (20:80)	20	170	Co-rotating
c-PHB/a-PHB (70:30)	20	170	Co-rotating
c-PHB/a-PHB (80:20)	20	170	Co-rotating
c-PHB/a-PHB (90:10)	20	170	Co-rotating
c-PHB*	20	170	Co-rotating
a-PHB + ESO/SA	20/100**	170	Co-rotating
PHBV/a-PHB (20:80) + ESO/SA	20/100**	170	Co-rotating
PHBV + DHPS	20/100**	160	Co-rotating
a-PHB + DHPS*	20/100**	170	Co-rotating
PHBV/a-PHB (20:80) + ESO/SA + DHPS	20/100**	170	Co-rotating
a-PHB + ESO/SA + DHPS	20/100**	170	Co-rotating
PHBV/a-PHB (20:80) + CaCO <sub>3</sub> /DCP	100/100**	180	Counter-rotating

\* Experiment performed by M. Bustos [111].

\*\* Initial / recycle.

The content of the additives in the blends was expressed as parts per hundred rubber (PHR), which is a convention often utilized in the plastics industry to describe the polymer ingredients as parts per hundred parts by weight of the polymer. A plasticizer content of 40 PHR, for example, represents the addition of 40 parts per 100 parts by weight of the polymer, which means a plasticizer composition of 28.6 wt%. To ensure the homogeneity of the blends when blending solid resins with liquid additives, extrusion was carried in multiple steps, where the extrudate of each batch was collected, chopped into small pieces, as shown in Figure 4.2, then recycled through the extruder after an overnight vacuum oven drying.



(a)

(b)

**Figure 4.2** – Collection of extrudate: (a) extrudate coming out from extruder; (b) chopped extrudate to be utilized in hot-press molding.

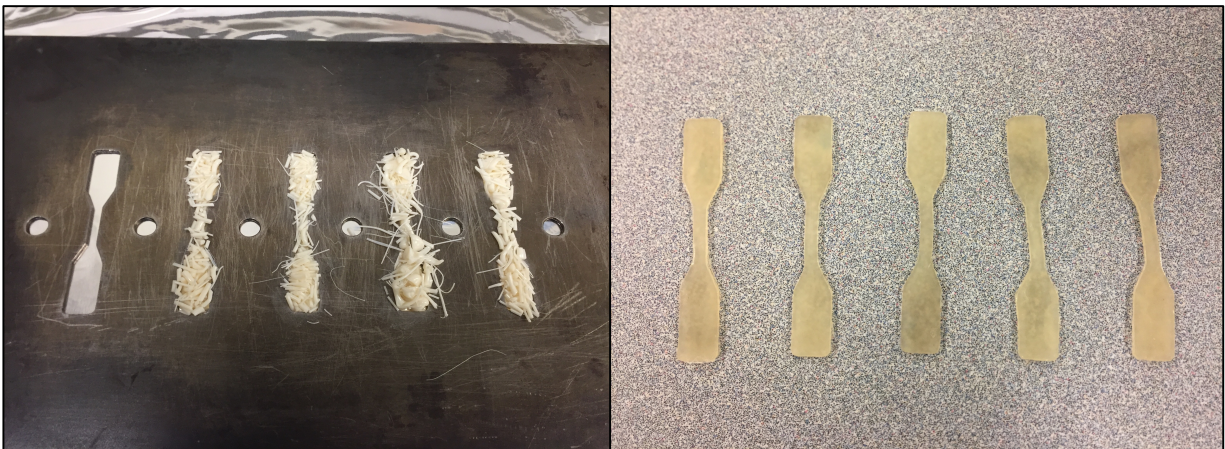
#### 4.3.2 Hot-Press Molding

The tensile test bars were made using a hot-press molding machine (Carver Manual Hydraulic Press with Watlow Temperature Controllers, Model #3856, Carver Inc.), shown in Figure 4.3. The steel mold was filled with chopped pieces of blend extrudate, as shown in Figure 4.4, and placed between two steel plates wrapped with aluminum foil, which was used to avoid contaminations which could result from direct contact of the polymer with the steel plates.





**Figure 4.3** – Hot-press molding machine (Carver Manual Hydraulic Press with Watlow Temperature Controllers, Model #3856, Carver Inc.).



(a)

(b)

**Figure 4.4** – Preparation of tensile test bars: (a) steel molds filled with chopped extrudate; (b) collected tensile bars after hot-press molding.

The applied pressure was measured from the pressure force over the area of the mold. The hot-press temperature was selected to match the extrusion temperature of each blend as per Table 4.2. The system heated up to the operating temperature for 3 min after placing the mold plates between the hot press plates, with contact at minimal pressure. Subsequently, a force of 0.5 MPa was applied for 5 min, followed by 1 MPa for 5 min, followed by 2 MPa for 10 min. Cyclic loading of 0 – 0.3 MPa was applied in between to remove any bubbles. Once completed, pressure was kept at 2 MPa and the cooling water supply was turned on to quench the samples and minimize crystallization of the polymers. The test bars were then removed from the mold and stored in a desiccator (Drierite, Fisher Scientific, Montréal, QC) at room temperature for 2 days prior to tensile strength testing. The dimensions of tensile test bars, shown in Figure 4.5, were in accordance with ASTM D-638 (2003) [112].

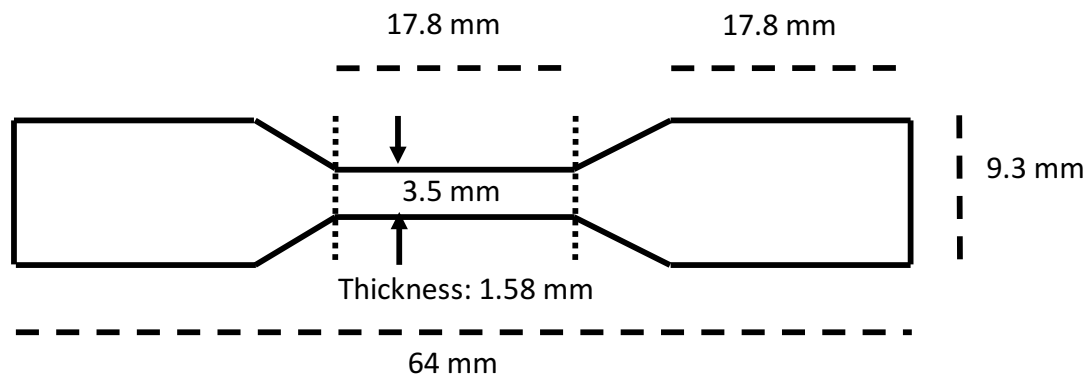


**Figure 4.5** – Dimensions of tensile testing bars in accordance to ASTM D-638 (2003) [112].

#### 4.3.3 Tensile Strength Testing

Tensile testing on the produced tensile test bars was performed in accordance to ASTM D-638 (2003) [112] using a compact table-top tensile strength tester (Shimadzu EZ Test) equipped with a 500 N load cell, shown in Figure 4.6. The tensile strength testing was performed on 3 tensile bars for each sample. A digital caliper (Fowler Tools and



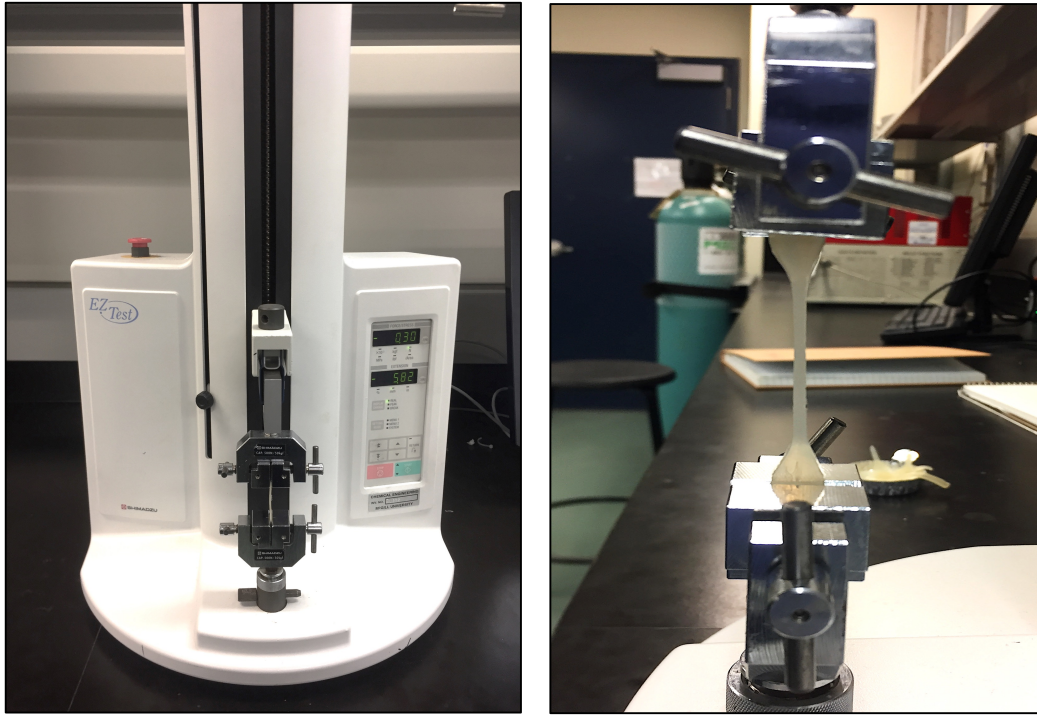


**Figure 4.6** – Tensile strength tester (Shimadzu EZ Test).

Instruments) was used to measure the initial width ( $W_0$ ) and initial thickness ( $T_0$ ) of the middle section of each tensile test bar, representing its cross-sectional area, and the initial distance between the metal grips of the tensile tester ( $L_0$ ). After manual measurement of the specimen dimensions and input of measurements into the software, the tensile test bars were attached to the equipment by fitting the grips into the apparatus and clamping them tight enough to ensure no slippage occurs during testing. A strain rate of 5 mm/min was utilized for tensile testing, and the tensile force applied by the tensile tester ( $F$ ) at corresponding distance ( $L$ ) was automatically recorded from the start of the test till specimen fracture.

The Shimadzu EZ software utilized the experimental data and the input measurements to generate a data spreadsheet with tensile stress and tensile strain data points at each distance, calculated in conjunction with (Eq. 1) and (Eq. 2):

$$\text{Elongation (\%)} = \frac{L - L_o}{L_o} \times 100 \left( \frac{mm}{mm} \right) \quad (\text{Eq. 1})$$

$$\text{Tensile Stress (MPa)} = \frac{F}{T_o \times W_o} \left( \frac{N}{mm^2} \right) \quad (\text{Eq. 2})$$

The calculated tensile stress and tensile strain data points were then plotted to produce a stress-strain curve. The stress-strain curve was utilized to determine the elongation at break (representing the maximum elongation till point of fracture), tensile strength (representing the maximum tensile stress achieved by the material), and the elastic modulus (corresponding to the slope of the stress-strain graph prior to the elastic region). The elastic modulus was determined using the derivative of the polynomial curve fit ( $R^2 > 98\%$ ) and was utilized to evaluate the flexibility of the polymer blend.

#### 4.4 Replicates

In this study, the amount of polymer resins used for each blend was a total of 9 grams, extruded in 3 consequent batches of 3 grams/batch. This amount of polymer resins was selected such that it was sufficient amount to produce 5 tensile bars specimen for tensile testing. However, several processing difficulties were faced when dealing with the PHA resins, mostly due to their sticky nature or weak strength. More specifically, the removal of the tensile bars specimen from the steel molds required inducing a minimal stress on the edges of each tensile bar to force it out. Such induced stress resulted in physical damage of some specimen represented by one or more tiny fractures at the edges of the central part of the tensile bars specimen. Such damaged specimens were discarded prior to tensile testing and, thus, testing was only performed using the other undamaged specimens. Moreover, some specimens were found to have fractures resulting from pre-existing tiny fractures that were not observed visually prior to tensile testing, but only during tensile testing upon stretching of the material. Such specimens often resulted in premature fracture and were discarded. At a later stage in this project, an inert silicon mold lubricant was sprayed on the steel molds prior to applying the extrudate into the molds. The lubricant reduced the stickiness of the

polymer blends to the molds, and reduced the instances of specimen damage. However, polymer blends with high compositions of  $\alpha$ -PHB were often very soft and sticky. On average, 3 specimens were obtained for each blend. The tensile testing results of these specimens were used to calculate statistically significant differences based on two-tailed t-test method. Differences with  $p < 0.1$  were considered statistically significant.

## 5. RESULTS

### 5.1 $^1\text{H}$ NMR Composition Analysis

The 300 MHz  $^1\text{H}$  NMR spectrum for the PHBV sample was well resolved, as shown in Figure 5.1. The HV content in PHBV was determined from the areas under the peaks of the methyl, ethyl and propyl groups resonances of the HV and HB repeating units, and was found to range between 14 – 15 mol% HV. Ideally, the area under the peak of the methylene resonance of the HV ethyl side group can be used in composition calculation. However, this is not advised as water presence in the copolymer or the solvent leads to an impurity at 1.67 ppm, causing an overlap with the methylene resonance of the HV unit in d-chloroform, which could lead to misleading higher HV unit compositions.

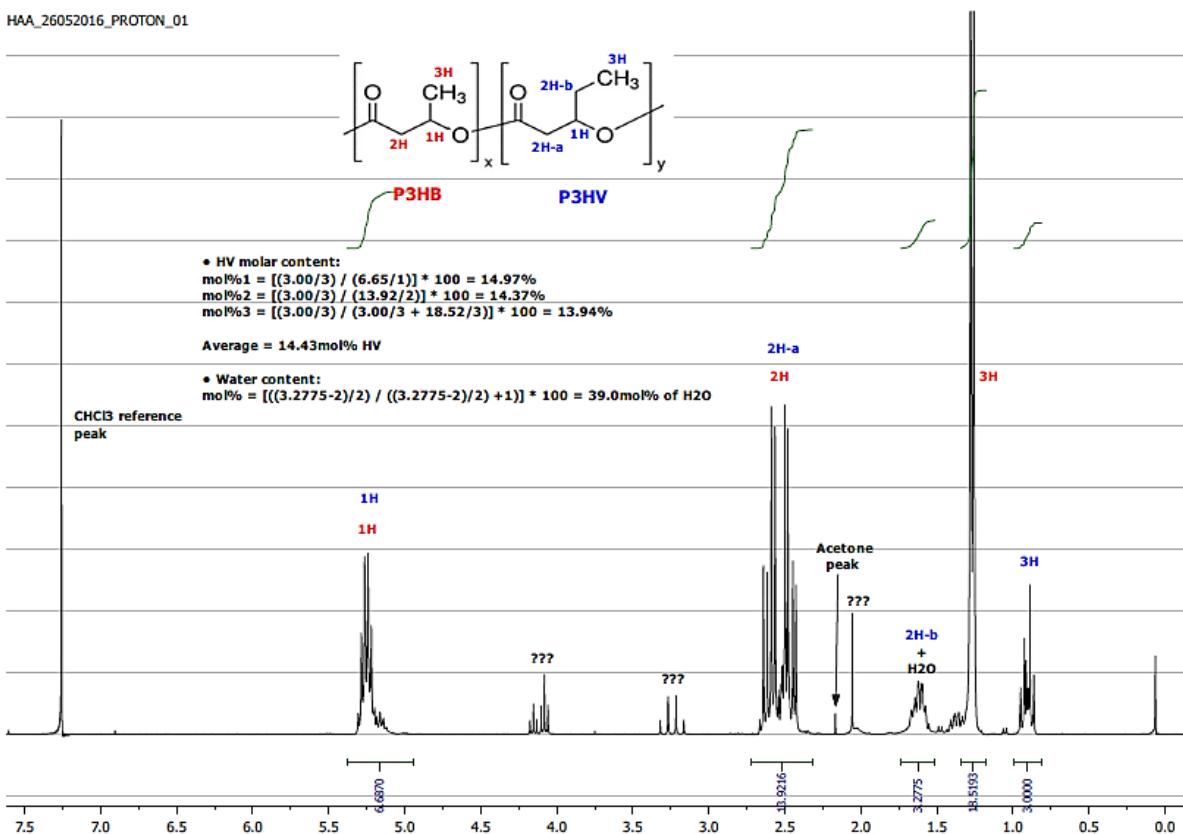
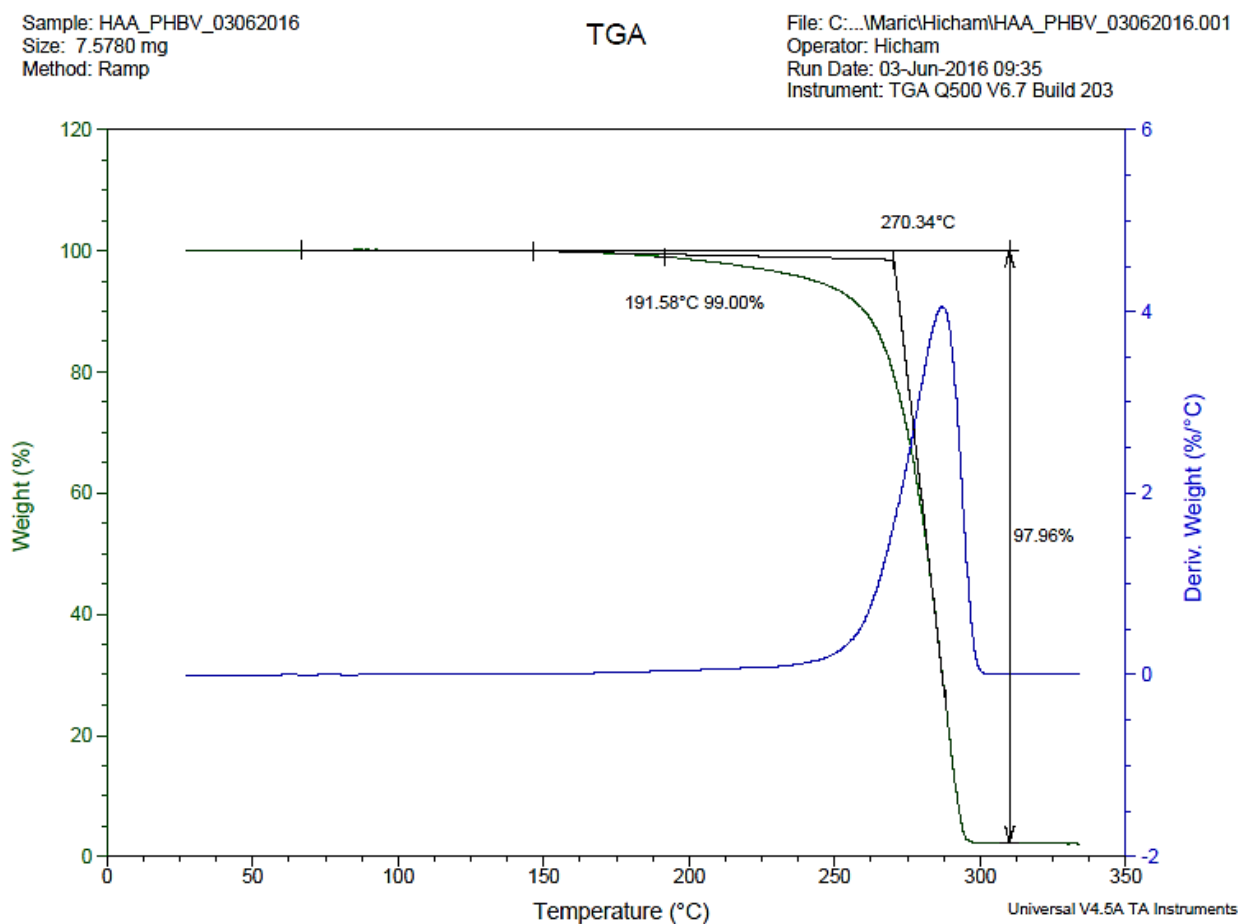


Figure 5.1 – NMR spectrum of PHBV sample.

## 5.2 Thermogravimetric Analysis

The TGA curve of the studied PHBV copolymer sample is shown in Figure 5.2. Material loss in the sample was first observed at temperatures above 160 °C with a 1 wt% material loss at 191 °C. The onset temperature, i.e. the temperature at which PHBV is 50% degraded, was found to be 270 °C which corresponds to the onset temperature found in literature [113]. PHBV is known to follow a random chain scission degradation mechanism which involves a  $\beta$ -hydrogen elimination process forming substrates of olefins and oligomers [114,115].



**Figure 5.2** – TGA plots of PHBV sample.

### 5.3 Neat Polymers and Neat Polymer Blends

The mechanical and thermal properties of the neat polymers and neat polymer blends were examined by tensile testing and differential scanning calorimetry (DSC). Neat polymer blends were prepared by melt extrusion of different polymers at various compositions, expressed in terms of wt%. The stress-strain curves and mechanical properties of the neat polymers and neat polymer blends are shown in Figure 5.3 and Table 5.1, respectively, while the DSC curves and thermal properties are shown in Figure 5.4 and Table 5.2, respectively.

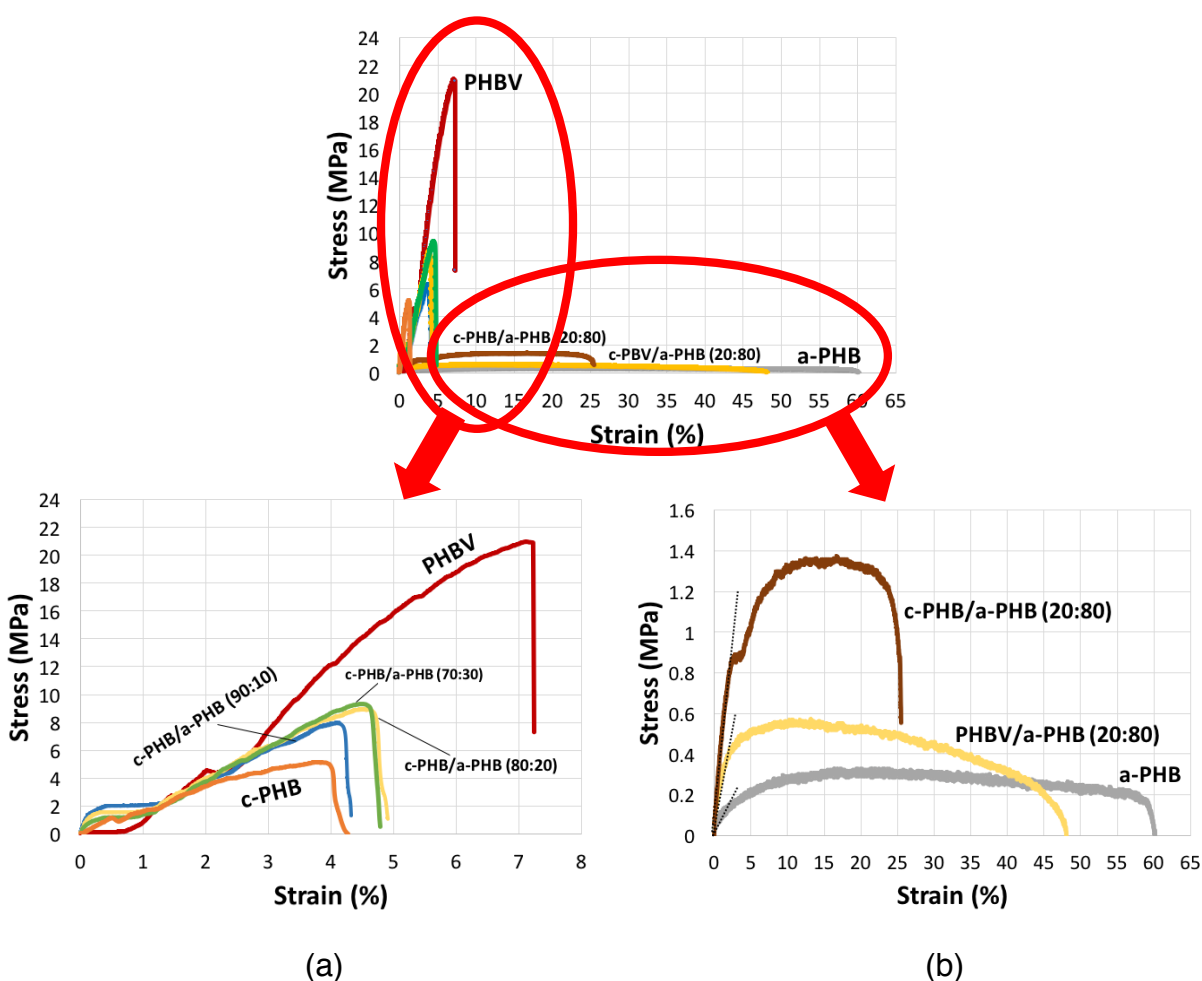


**Figure 5.3** – Typical stress-strain curves of neat polymers and neat polymer blends: (a) c-PHB, c-PHB/a-PHB (90:10), c-PHB/a-PHB (80:20), c-PHB/a-PHB (70:30), PHBV; (b) c-PHB/a-PHB (20:80), PHBV/a-PHB (20:80), a-PHB.

**Table 5.1** – Mechanical properties of neat polymers and neat polymer blends.

Blends	Tensile Strength	Elongation at Break	Elastic Modulus
	(MPa)	(%)	(MPa)
PHBV	$21.08 \pm 0.62$	$7.5 \pm 0.7$	$531.2 \pm 19.0$
a-PHB*	$0.33 \pm 0.01$	$65.3 \pm 5.1$	$7.3 \pm 1.3$
PHBV/a-PHB (20:80)	$0.62 \pm 0.06$	$43.9 \pm 3.1$	$22.2 \pm 14.2$
c-PHB/a-PHB (20:80)	$1.33 \pm 0.04$	$28.1 \pm 2.6$	$38.9 \pm 2.7$
c-PHB/a-PHB (70:30)	$9.32 \pm 1.50$	$5.0 \pm 0.4$	$232.1 \pm 24.7$
c-PHB/a-PHB (80:20)	$8.97 \pm 0.27$	$4.8 \pm 0.4$	$248.3 \pm 9.1$
c-PHB/a-PHB (90:10)	$8.48 \pm 0.86$	$5.5 \pm 0.4$	$248.1 \pm 14.2$
c-PHB*	$5.08 \pm 0.47$	$4.0 \pm 0.2$	$233.0 \pm 31.9$

\*Experimental data obtained from M. Bustos [111].

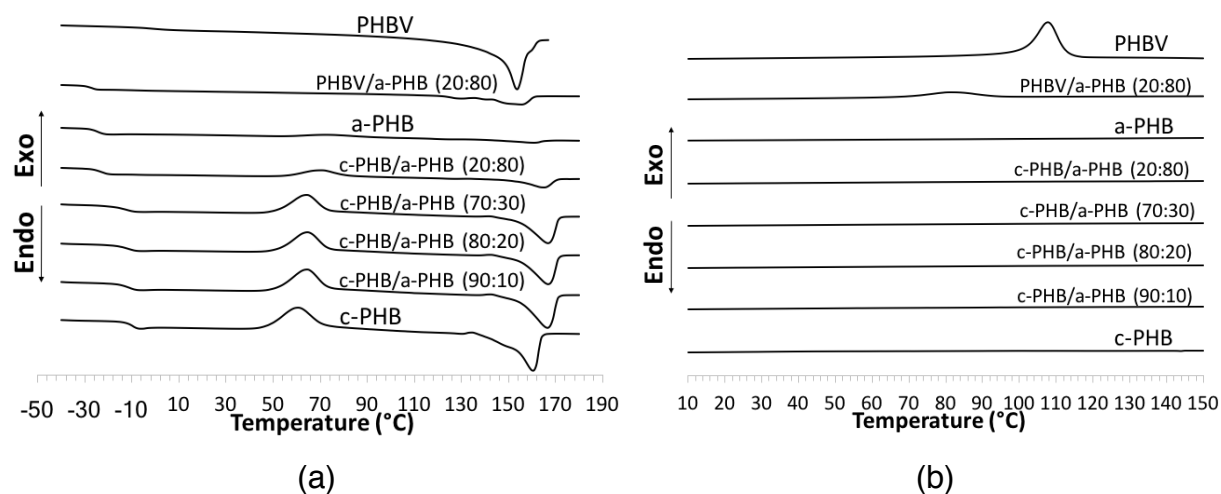


**Figure 5.4** – DSC curves of neat polymers and neat polymer blends: (a) second heating cycle; (b) cooling cycle.

**Table 5.2** – Thermal properties of neat polymers and neat polymer blends.

Blends	$T_g$	$T_c$	$\Delta H_c$	$T_m$	$\Delta H_m$
	(°C)	(°C)	(J/g)	(°C)	(J/g)
PHBV	-3.4	107.7	52.2	153.7	64.3
a-PHB*	-24.5	-	-	161.0	3.0
PHBV/a-PHB (20:80)	-26.4	81.3	12.9	155.5	14.5
c-PHB/a-PHB (20:80)	-22.4	-	-	165.2	10.0
c-PHB/a-PHB (70:30)	-12.6	-	-	167.0	29.1
c-PHB/a-PHB (80:20)	-11.1	-	-	166.9	31.6
c-PHB/a-PHB (90:10)	-10.6	-	-	166.6	35.7
c-PHB*	-9.3	-	-	160.3	38.9

\*Experimental data obtained from M. Bustos [111].

#### 5.4 Plasticizing with ESO and SA

The effect of the addition of ESO and SA on the mechanical and thermal properties of the neat polymer blends was examined through tensile strength and DSC testing. The effects of the addition of 5 PHR of ESO and 1 PHR of SA on the elongation break and tensile strength of a-PHB and PHBV/a-PHB (20:80) are shown in Figure 5.5. The mechanical properties for blends plasticized with ESO and SA are shown in Table 5.3, while the DSC curves and thermal properties are shown in Figure 5.6 and Table 5.4, respectively.



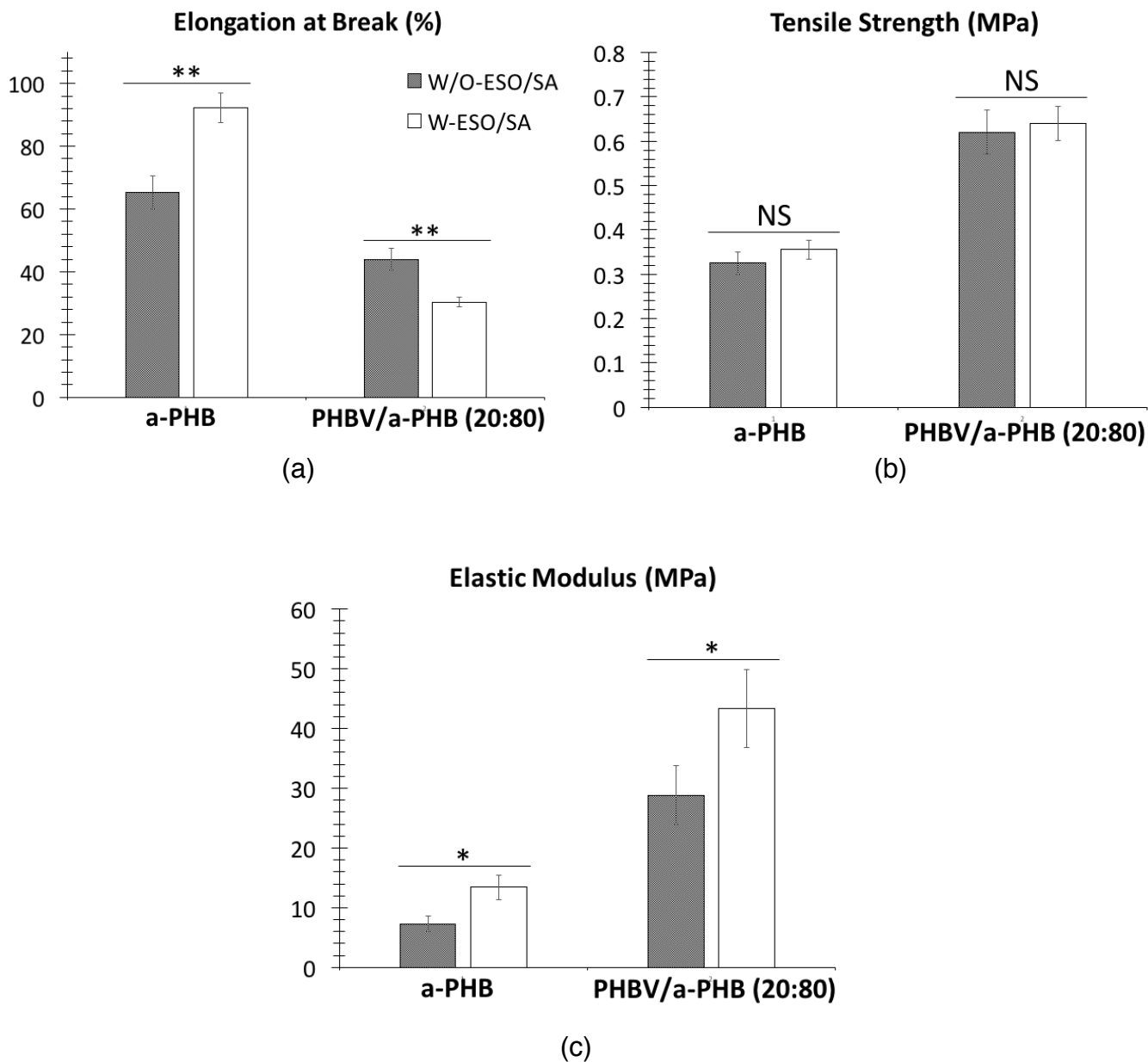


**Figure 5.5** – Tensile effects of ESO and SA on blends: (a) elongation at break (%): a-PHB (t-test,  $p < 0.05$ ), PHBV/a-PHB (20:80) (t-test,  $p < 0.05$ ); (b) tensile strength (MPa): a-PHB (t-test,  $p > 0.1$ ), PHBV/a-PHB (20:80) (t-test,  $p > 0.1$ ); (c) elastic modulus (MPa): a-PHB (t-test,  $p = 0.09$ ), PHBV/a-PHB (20:80) (t-test,  $p = 0.07$ ).

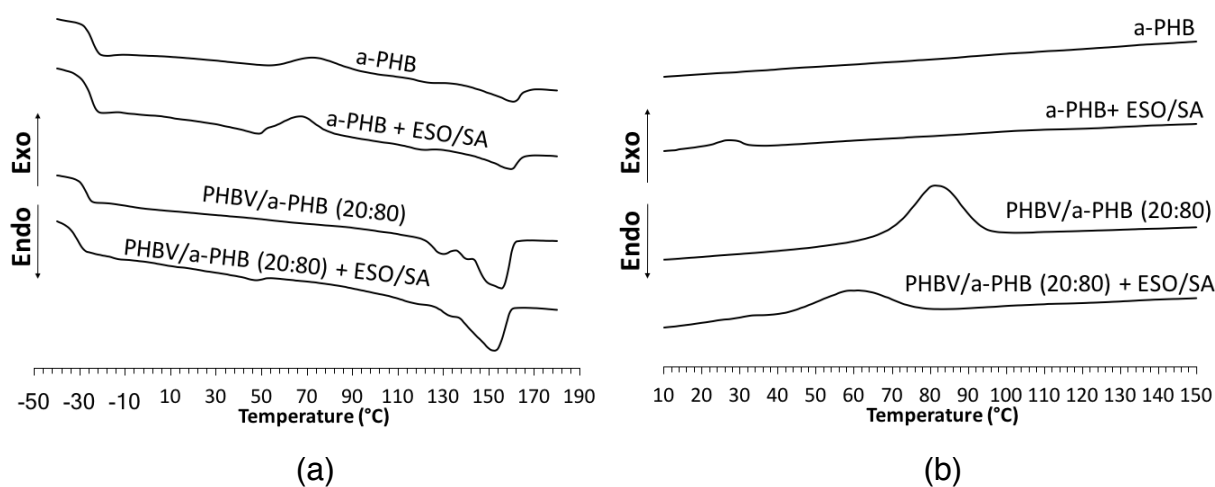
*W: with 5 PHR ESO and 1 PHR SA, W/O: without ESO and SA. Error bars represent  $\pm$  standard deviation. Asterisks indicate significant differences:*

*(NS):  $p > 0.1$ , (\*):  $p < 0.1$ , (\*\*):  $p < 0.05$ .*

**Table 5.3** – Mechanical properties of blends with ESO and SA.

Blends	ESO	SA	Tensile Strength	Elongation at Break	Elastic Modulus
	(PHR)	(PHR)	(MPa)	(%)	(MPa)
a-PHB*	-	-	$0.33 \pm 0.01$	$65.3 \pm 5.1$	$7.3 \pm 1.3$
a-PHB + ESO/SA	5	1	$0.36 \pm 0.02$	$92.3 \pm 4.6$	$13.4 \pm 1.0$
PHBV/a-PHB (20:80)	-	-	$0.62 \pm 0.05$	$43.9 \pm 3.1$	$22.2 \pm 14.2$
PHBV/a-PHB (20:80) + ESO/SA	5	1	$0.64 \pm 0.04$	$30.4 \pm 0.6$	$43.4 \pm 6.7$

\*Experimental data obtained from M. Bustos [111].

**Figure 5.6** – DSC curves of blends with ESO and SA: (a) second heating cycle; (b) cooling cycle.

*Additives composition: 5 PHR ESO, 1 PHR SA.*

**Table 5.4** – Thermal properties of blends with ESO and SA.

Blends	ESO	SA	T <sub>g</sub>	T <sub>c</sub>	ΔH <sub>c</sub>	T <sub>m</sub>	ΔH <sub>m</sub>
	(PHR)	(PHR)	(°C)	(°C)	(J/g)	(°C)	(J/g)
a-PHB*	-	-	-24.5	-	-	161.0	3.0
a-PHB + ESO/SA	5	1	-24.8	-	-	160.0	3.2
PHBV/a-PHB (20:80)	-	-	-26.4	81.3	12.9	155.5	14.5
PHBV/a-PHB (20:80) + ESO/SA	5	1	-30.9	60.5	7.3	152.7	11.5

\*Experimental data obtained from M. Bustos [111].

## 5.5 Plasticizing with DHPS

The effect of the addition of DHPS on the mechanical and thermal properties of the neat polymer blends was examined through tensile strength and DSC testing. The effects of the addition of 40 PHR DHPS on the elongation at break and tensile strength of the polymers are shown in Figure 5.7. The mechanical properties for blends plasticized with DHPS are shown in Table 5.5, while the DSC curve and thermal properties for one of the blends is shown in Figure 5.8 and Table 5.6, respectively.

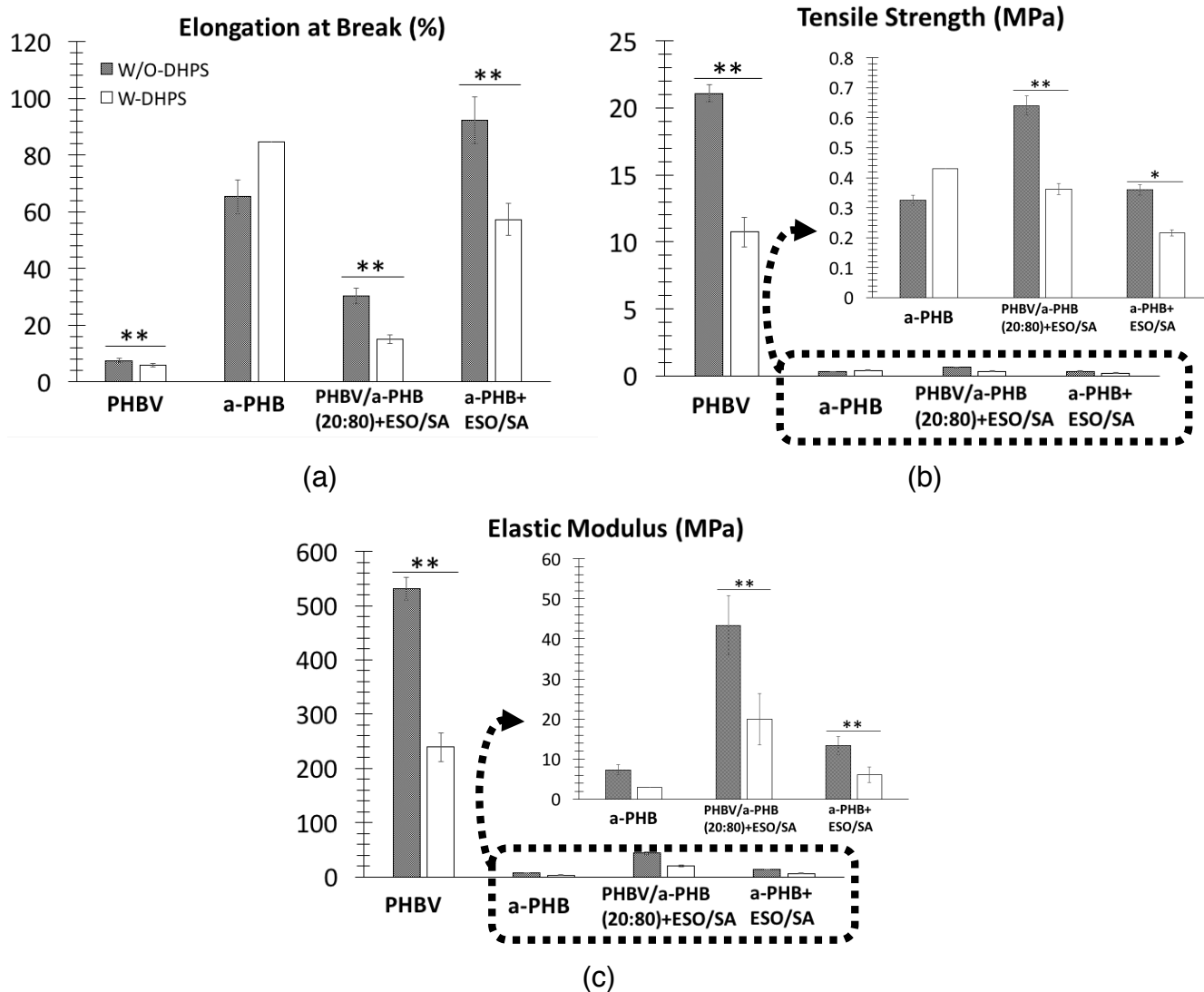


**Figure 5.7** – Tensile effects of DHPS on blends: (a) elongation at break (%): PHBV (t-test,  $p < 0.05$ ), a-PHB [111], PHBV/a-PHB (20:80)+ESO/SA (t-test,  $p < 0.05$ ), a-PHB+ESO/SA (t-test,  $p < 0.05$ ); (b) tensile strength (MPa): PHBV (t-test,  $p < 0.05$ ), a-PHB [111], PHBV/a-PHB (20:80)+ESO/SA (t-test,  $p < 0.05$ ), a-PHB+ESO/SA (t-test,  $p < 0.1$ ); (c) elastic modulus (MPa): PHBV (t-test,  $p < 0.05$ ), a-PHB [111], PHBV/a-PHB (20:80)+ESO/SA (t-test,  $p < 0.05$ ), a-PHB+ESO/SA (t-test,  $p < 0.05$ ).

*Additives composition: 5 PHR ESO, 1 PHR SA, 40 PHR DHPS. Error bars represent  $\pm$  standard deviation. Asterisks indicate significant differences: (\*) :  $p < 0.1$ , (\*\*) :  $p < 0.05$ .*

**Table 5.5** – Mechanical properties of blends with DHPS.

Blends	ESO	SA	DHPS	Tensile Strength	Elongation at Break	Elastic Modulus
	(PHR)	(PHR)	(PHR)	(MPa)	(%)	(MPa)
PHBV	-	-	-	21.08 ± 0.62	7.5 ± 0.7	531.2 ± 19.0
PHBV + DHPS	-	-	40	10.73 ± 0.11	5.8 ± 0.1	239.2 ± 8.2
a-PHB*	-	-	-	0.33 ± 0.01	65.3 ± 5.1	7.3 ± 1.3
a-PHB + DHPS* **	-	-	40	0.43 ± 0.00	84.6 ± 0.0	2.9 ± 0.0
PHBV/a-PHB (20:80) + ESO/SA	5	1	-	0.64 ± 0.04	30.4 ± 0.6	43.4 ± 6.7
PHBV/a-PHB (20:80) + ESO/SA + DHPS	5	1	40	0.36 ± 0.02	15.1 ± 0.2	20.0 ± 6.4
a-PHB + ESO/SA	5	1	-	0.36 ± 0.02	92.3 ± 4.6	13.4 ± 1.0
a-PHB + ESO/SA + DHPS	5	1	40	0.22 ± 0.01	57.3 ± 5.4	6.1 ± 0.7

\*Experimental data obtained from M. Bustos [111].

\*\*Number of tested samples=1.

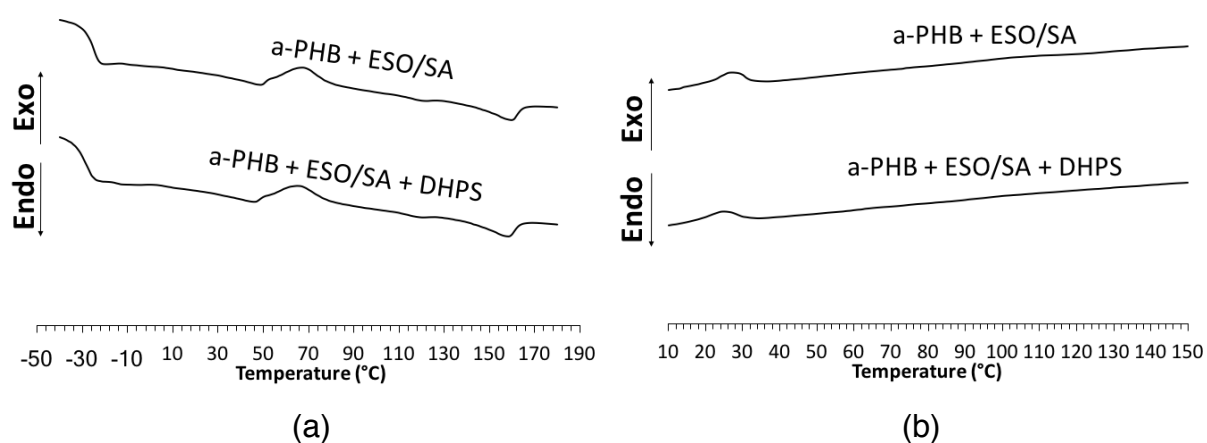


**Figure 5.8** – DSC curves of blend plasticized with DHPS: (a) second heating cycle; (b) cooling cycle.

*Additives composition: 5 PHR ESO, 1 PHR SA, 40 PHR DHPS.*

**Table 5.6** – Thermal properties of blends with DHPS.

Blends	ESO	SA	DHPS	T <sub>g</sub>	T <sub>c</sub>	ΔH <sub>c</sub>	T <sub>m</sub>	ΔH <sub>m</sub>
	(PHR)	(PHR)	(PHR)	(°C)	(°C)	(J/g)	(°C)	(J/g)
a-PHB + ESO/SA	5	1	-	-24.8	-	-	160.0	3.2
a-PHB + ESO/SA + DHPS	5	1	40	-28.4	-	-	158.4	3.2

## 5.6 Crosslinking using DCP and Filling with CaCO<sub>3</sub>

The effect of the addition of DHPS on the mechanical and thermal properties of a neat polymer blend, PHBV/a-PHB (20:80), was examined through tensile strength and DSC testing. The effect of the addition of 10 PHR of CaCO<sub>3</sub> and 1 PHR of DCP on the stress-strain curve of the polymer blend is shown in Figure 5.9. The mechanical properties for a blend filled with CaCO<sub>3</sub> and crosslinked using DCP and is shown in Table 5.7, while the DSC curve and thermal properties is shown in Figure 5.10 and Table 5.8, respectively.

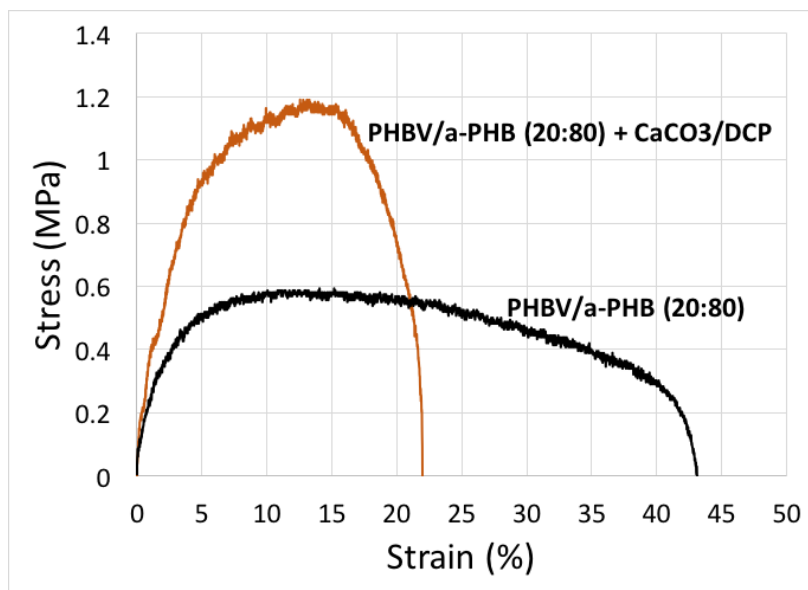


**Figure 5.9** – Tensile effects of DCP/CaCO<sub>3</sub> on typical stress-strain curve.

*Additives composition: 1 PHR DCP, 10 PHR CaCO<sub>3</sub>.*

**Table 5.7** – Mechanical properties of blends with DCP/CaCO<sub>3</sub>.

Blends	CaCO <sub>3</sub>	DCP	Tensile Strength	Elongation at Break	Elastic Modulus
	(PHR)	(PHR)	(MPa)	(%)	(MPa)
PHBV/a-PHB (20:80)	-	-	0.62 ± 0.06	43.9 ± 3.1	22.2 ± 14.2
PHBV/a-PHB (20:80) + CaCO <sub>3</sub> /DCP	10	1	1.43 ± 0.21	24.0 ± 2.8	65.1 ± 12.6

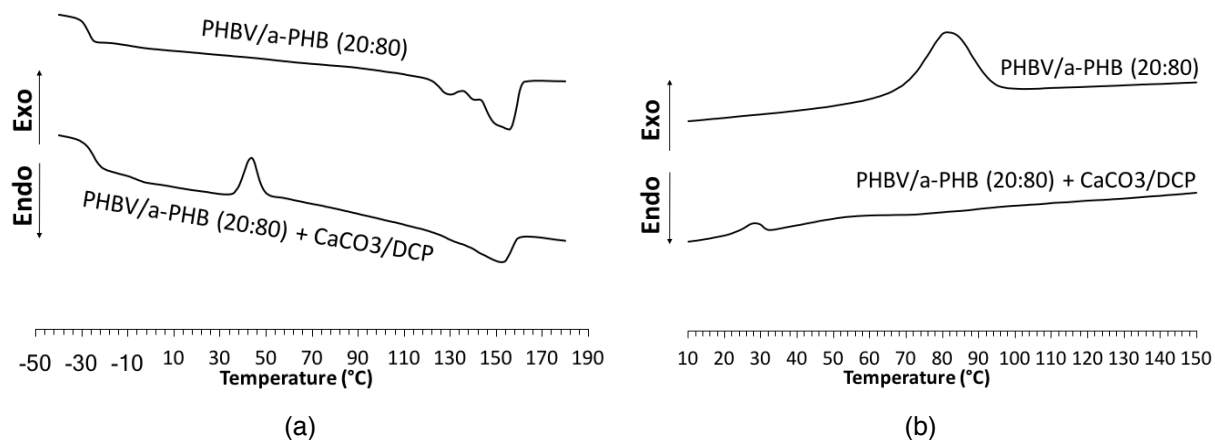


**Figure 5.10** – DSC curves of blend with DCP/CaCO<sub>3</sub>: (a) second heating cycle; (b) cooling cycle.

*Additives composition: 1 PHR DCP, 10 PHR CaCO<sub>3</sub>.*

**Table 5.8** – Thermal properties of blends with DCP/CaCO<sub>3</sub>.

Blends	CaCO <sub>3</sub>	DCP	T <sub>g</sub>	T <sub>c</sub>	ΔH <sub>c</sub>	T <sub>m</sub>	ΔH <sub>m</sub>
	(PHR)	(PHR)	(°C)	(°C)	(J/g)	(°C)	(J/g)
PHBV/a-PHB (20:80)	-	-	-26.4	81.3	12.9	155.5	14.5
PHBV/a-PHB (20:80) + CaCO <sub>3</sub> /DCP	10	1	-24.5	-	-	152.1	7.3

## 6. DISCUSSION

PHBV, c-PHB and a-PHB had varying mechanical properties in terms of their elasticity, toughness and flexibility, and varying thermal properties in terms of their  $T_m$ ,  $T_g$  and crystallization isotherm. PHBV exhibited brittle characteristics with superior tensile strength compared to c-PHB and a-PHB, while a-PHB exhibited amorphous characteristics with superior elongation at break, but inferior tensile strength, compared to PHBV and c-PHB. This study represents the first attempt to study the effects of polymer blending of different PHA resins with each other. Blends prepared using different compositions of these polymers had intermediate mechanical and thermal properties, except for blends with 10 – 30 wt% of a-PHB in c-PHB, in which improved toughness was observed. The addition of 10 – 30 wt% of a-PHB into c-PHB resulted in blends with higher tensile strength compared to both, neat c-PHB and neat a-PHB (t-test,  $p < 0.05$ ). These results demonstrate the ability to control the mechanical and thermal properties of different PHA resins, which can stimulate future work in selecting optimum compositions of polymer blends that provide maximum compatibility with plasticizers.

This study also represents the first attempt to use ESO, SA and the novel ‘green’ plasticizer, DHPS, to plasticize polymer blends made from different PHA resins. ESO/SA and DHPS had consistent opposing effects on flexibility of the polymers, in which the addition of ESO/SA resulted in blends with slightly lower flexibility (t-test,  $p = 0.09$ ), while the addition of DHPS resulted in blends with higher flexibility (t-test,  $p < 0.05$ ). ESO/SA was successful in plasticizing a-PHB, in which the addition of 5 PHR ESO and 1 PHR SA increased its elongation at break from 65% to 92% (t-test,  $p < 0.05$ ), and increased its elastic modulus from 7 MPa to 13 MPa (t-test,  $p < 0.05$ ). However, the addition of ESO/SA to blends composed of 20% wt PHBV and 80 wt% a-PHB resulted in blends with lower elongation at break and a modified crystallization mechanism, in which the plasticized blends exhibited retarded crystallization. The addition of 5 PHR ESO and 1 PHR SA to blends composed of 20 wt% PHBV and 80 wt% a-PHB decreased their  $T_c$  from 81 °C to 61 °C, and decreased their  $\Delta H_c$  from 13 J/g to 7 J/g



compared to neat polymer blends, with no detected cold crystallization in both, plasticized blends and neat polymer blends. Moreover, preliminary results showed that DHPS was also successful in plasticizing a-PHB, in which the addition of 40 PHR DHPS to a-PHB increased its elongation from 65% to 85%, decreased its elastic modulus from 7 MPa to 3 MPa, and increased its tensile strength from 0.3 MPa to 0.4 MPa. These results demonstrate the possibility to plasticize PHA resins using bio-based plasticizers, which can stimulate future work to better understand the parameters affecting the degree of plasticization, and ultimately lead to the use of PHA in novel bioplastic applications, in which non-toxic, biocompatible and completely biodegradable plastics are desired.

Finally, DCP/CaCO<sub>3</sub> exhibited typical toughening effects at the cost of elongation at break, in which the addition of 1 PHR DCP and 10 PHR CaCO<sub>3</sub> resulted in blends with higher tensile strength, lower elastic modulus and lower elongation at break (t-test,  $p < 0.05$ ). These effects were accompanied with a modified crystallization mechanism, in which the addition of CaCO<sub>3</sub>/DCP eliminated the crystallization peak which was observed in the cooling isotherm of PHBV/a-PHB (20:80) at  $T_c$  of 81 °C, and resulted in blends with a completely flat crystallization isotherm.

## **6.1 Neat Polymers and Neat Polymer Blends**

PHBV and c-PHB were very brittle and exhibited no plastic deformation, while a-PHB exhibited plastic deformation with a higher elongation at break, but at the cost of tensile strength. PHBV exhibited a higher tensile strength compared to both, c-PHB and a-PHB. The tensile strength of PHBV was 21 MPa, while the tensile strengths of c-PHB and a-PHB were 5 MPa and 0.3 MPa, respectively. The elongation at break of a-PHB was 65%, while the elongation at break values of PHBV and c-PHB were 8% and 4%, respectively. As shown in Figure 5.3, there was a clear trade-off between elongation at break and tensile strength of a-PHB and c-PHB, with a-PHB exhibiting higher elongation at break, but lower tensile strength than c-PHB. The  $T_g$  of a-PHB was considerably lower

than those of PHBV and c-PHB. The  $T_g$  of a-PHB was  $-25\text{ }^{\circ}\text{C}$ , while the  $T_g$  values of PHBV and c-PHB were  $-3\text{ }^{\circ}\text{C}$  and  $-9\text{ }^{\circ}\text{C}$ , respectively. The  $T_g$  values are consistent with the tensile results, in which softer polymers had lower  $T_g$  values. a-PHB had an elastic modulus of 7 MPa, while PHBV and c-PHB had elastic moduli of 530 MPa and 230 MPa, respectively. The measured elongation at break, tensile strength and  $T_g$  for PHBV and c-PHB are consistent with values reported in literature [14,84,116–120]. As shown in Table 5.2, no melt crystallization isotherms were detected for a-PHB, c-PHB and blends of both. This indicates that the blends were either amorphous or have a slow nucleation rate that is accompanied with depletion of crystallizable molecules and spherulitic impingement [121–123]. Similar results were obtained for c-PHB by *Wellen et al*, where the crystallization isotherm was found to either have a sigmoid shape or be completely flat with no detected crystallization temperature ( $T_c$ ), depending on the cooling rate the polymer was exposed to [120].

The melt blending of 20 wt % a-PHB with either PHBV or c-PHB generally resulted in blends with intermediate mechanical and thermal properties. The addition of 20 wt% PHBV to a-PHB resulted in intermediate elongation at break, tensile strength, elastic modulus and  $T_m$  values compared to both, neat PHBV and neat a-PHB, with no significant effects on  $T_g$  compared to a-PHB. The addition of 20 wt% c-PHB to a-PHB resulted in similar intermediate elongation at break, tensile strength, elastic modulus values compared to both, neat c-PHB and neat a-PHB, with similar no significant effects on  $T_g$  compared to neat a-PHB; however, it resulted in blends with higher  $T_m$  values compared to both, neat c-PHB and neat a-PHB. The addition of 20 wt% c-PHB to a-PHB resulted in blends with  $T_m$  values of  $165\text{ }^{\circ}\text{C}$ , while the  $T_m$  values of neat c-PHB and neat a-PHB were  $160\text{ }^{\circ}\text{C}$  and  $161\text{ }^{\circ}\text{C}$ , respectively. It can also be observed from the stress versus strain curves, shown in Figure 5.3–(b), that both, the addition of 20 wt% PHBV to a-PHB and the addition of 20 wt% c-PHB to a-PHB produced blends that yielded at a very low strain and exhibited a plastic deformation similar to a-PHB. The addition of 20 wt% c-PHB to a-PHB resulted in blends with lower elongation at break and higher tensile strength compared to blends with 20 wt% PHBV added to a-PHB (t-test,  $p < 0.05$ ), with no

significant effects on elastic modulus (t-test,  $p>0.05$ ). Blends with 20 wt% c-PHB added to a-PHB exhibited an elongation at break of 28% compared to 44% for blends with 20 wt% PHBV added to a-PHB, and tensile strength of 1.3 MPa compared to 0.6 MPa for blends with 20 wt% PHBV added to a-PHB. The melt blending of 10 – 30 wt% a-PHB with c-PHB resulted in blends with intermediate  $T_g$  values, and higher  $T_m$  values compared to neat c-PHB, with no significant effects on either elongation at break or elastic modulus compared to c-PHB (t-test,  $p>0.05$ ). However, the melt blending of 10 – 30 wt% a-PHB with c-PHB resulted in blends with higher tensile strength compared to both, neat c-PHB and neat a-PHB (t-test,  $p<0.05$ ). For example, the addition of 20 wt% a-PHB to c-PHB resulted in blends with tensile strength of 9 MPa, compared to 5 MPa for neat c-PHB and 0.3 MPa for neat a-PHB. As shown in Figure 5.4–(a), exothermic peaks in the heating cycles of c-PHB and c-PHB/a-PHB blends were observed at temperatures between 60 °C and 70 °C. These peaks represent the cold crystallization of c-PHB at which the chain segments have enough energy to become mobile and reorganize. Similar observations were observed by *Wellen et al*, in which the cold crystallization of c-PHB was found to be highly dependent on the heating rate the polymer is exposed to [120].

## 6.2 Plasticizing with ESO/SA

Melt blending of ESO and SA with a-PHB resulted in blends with higher elongation at break (t-test,  $p<0.05$ ) and lower flexibility (t-test,  $p=0.09$ ), with no significant effects on either tensile strength (t-test,  $p>0.1$ ),  $T_g$  or  $T_m$ . The addition of 5 PHR ESO and 1 PHR SA to a-PHB increased its elongation at break from 65% to 92%, and increased its elastic modulus from 7 MPa to 13 MPa. Such toughening and elastomeric effects can be attributed to favorable ESO interactions with polymers having an ester group via hydrogen bonding [76].

Similar toughening effects and slight reductions in  $T_g$  were observed upon the addition of ESO/SA to blends composed of 20 wt% PHBV and 80 wt% a-PHB. However, this was accompanied with undesired effects on elongation at break. The addition of 5

PHR ESO and 1 PHR SA to PHBV/a-PHB (20:80) increased its elastic modulus from 22 MPa to 43 MPa (t-test,  $p=0.07$ ), decreased its  $T_g$  from  $-26\text{ }^{\circ}\text{C}$  to  $-31\text{ }^{\circ}\text{C}$ , and decreased its elongation at break from 44% to 30% compared to the neat polymer blend (t-test,  $p<0.05$ ). The reduction in  $T_g$  is consistent with findings reported previously [84], in which the addition of 20 wt% ESO to PHBV (6 wt% HV) decreased its  $T_g$  from  $-6\text{ }^{\circ}\text{C}$  to  $-19\text{ }^{\circ}\text{C}$ , but with no significant effects on elongation at break.

A modification in the crystallization mechanism, represented by lower  $T_c$  and  $\Delta H_c$  values, was also observed upon the addition of ESO/SA to PHBV/a-PHB (20:80). The addition of 5 PHR ESO and 1 PHR SA to PHBV/a-PHB (20:80) decreased its  $T_c$  from  $81\text{ }^{\circ}\text{C}$  to  $61\text{ }^{\circ}\text{C}$ , and decreased its  $\Delta H_c$  from 13 J/g to 7 J/g compared to the neat polymer blend, with no detected cold crystallization in both, plasticized blends and neat polymer blends. Such retarded crystallization could be attributed to basic plasticizing effects, in which the plasticizer acts as a lubricant, and makes it harder for the polymers to crystallize. Moreover, a small endothermic peak was observed at a temperature of  $50 - 55\text{ }^{\circ}\text{C}$  in the heating isotherm of plasticized blends, as shown in Figure 5.6–(b). This endothermic peak can be attributed to the melting of SA, which has a  $T_m$  of  $69\text{ }^{\circ}\text{C}$ . Similarly, a small exothermic peak was observed at a temperature of  $30 - 35\text{ }^{\circ}\text{C}$  in the cooling isotherm of the plasticized blend, which can also be attributed to the crystallization of SA. Such observation could suggest a potential non-compatibility with either a-PHB or blends containing a-PHB. *Requena et al* observed similar  $T_m$  and  $T_c$  peaks with the addition of 10 wt% SA to PHBV [124]. The addition of 10 wt% SA to PHBV decreased its degree of crystallization 74% to 64%, and decreased its  $T_m$  from  $168\text{ }^{\circ}\text{C}$  to  $159\text{ }^{\circ}\text{C}$ , with no significant effects on either elongation at break or elastic modulus [124]. The degree of crystallinity of SA in the blend was estimated using the enthalpy value, as well as considering the melting enthalpy of crystallized SA ( $\Delta H_m = 230\text{ J/g}$ ) and its mass fraction in the blend [124]. The degree of crystallinity of SA in the blend increased from 42% to 62% after 5 weeks of ageing, in which SA progressively separated from the PHBV matrix and crystallized in a different phase [124].

To study the effectiveness of a plasticizer, it is essential to evaluate its compatibility and solubility with the polymer matrix. The solubility parameters of ESO, SA and the monomers of PHBV, c-PHB and a-PHB, shown in Table 6.1, were calculated using the Hoftyzer–Van Krevelen method [125]. This method is based on solubility parameter component group contributions, shown in Table A1 in Appendix A, which considers similarities in some chemical and physical properties of chemical compounds when found in different molecules. Each molecule of interest was analyzed and weighed with respect to the various chemical compounds forming the molecule. Component group contributions were then utilized to calculate the overall solubility parameter ( $\delta$ ), dispersion component ( $\delta_d$ ), polar component ( $\delta_p$ ) and hydrogen bonding component ( $\delta_h$ ). The detailed calculations are provided in Appendix A.

**Table 6.1** – Solubility parameters of polymers and ESO/SA including: overall solubility parameter ( $\delta$ ), dispersion component ( $\delta_d$ ), polar component ( $\delta_p$ ) and hydrogen bonding component ( $\delta_h$ ) of the polymers, ESO and SA.

Repeat Unit	$\delta$	$\delta_d$	$\delta_p$	$\delta_h$
	( $MPa^{1/2}$ )	( $MPa^{1/2}$ )	( $MPa^{1/2}$ )	( $MPa^{1/2}$ )
3HV	21.9	16.8	10.5	9.4
3HB	22.2	16.4	12.3	8.4
PHBV [84]	20.6	16.5	8.8	8.6
4HB	22.6	17.0	12.3	8.4
ESO	16.1	14.9	1.9	5.9
SA	18.7	16.5	2.9	8.3
ESO [84]	16.8	16.5	1.6	5.1
DBP [84]	19.1	17.9	4.1	5.3
TEC [84]	23.8	20.3	3.6	11.8

In general, compatibilization of a plasticizer requires similar solubility parameters between the polymer and the plasticizer, especially in its polar and hydrogen bonding components [126]. The calculated  $\delta$  of the polymers ranged between 21.9 and 22.6  $MPa^{1/2}$ , while  $\delta$  of ESO and SA were 16.1  $MPa^{1/2}$  and 18.7  $MPa^{1/2}$ , respectively. The  $\delta_d$  values of ESO and SA were relatively close to those of the polymers, while the  $\delta$  and  $\delta_h$

values were distant, with huge differences in  $\delta_p$  between the plasticizers and the polymers. Similar observations were made by *Choi and Park* when comparing the solubility parameters of PHBV, ESO, dibutyl phthalate (DBP) and triethyl citrate (TEC) [84]. The addition of 20 wt% DBP, with a  $\delta$  value of  $19.1 \text{ MPa}^{1/2}$  instead of ESO which has a  $\delta$  value of  $16.8 \text{ MPa}^{1/2}$ , into PHBV resulted in an elongation at break of 10% instead of 8%, a  $T_g$  of  $-29^\circ\text{C}$  instead of  $-19^\circ\text{C}$ , and a  $T_m$  of  $153^\circ\text{C}$  instead of  $160^\circ\text{C}$  [84]. Similarly, the addition of 20 wt% TEC, with a  $\delta$  value of  $23.8 \text{ MPa}^{1/2}$ , into PHBV resulted in an elongation at break of 10%, a  $T_g$  of  $-30^\circ\text{C}$ , and a  $T_m$  of  $144^\circ\text{C}$  [84]. Overall, lower  $T_g$ , higher impact strength and slightly higher elongation at break values were achieved with DBP and TEC, both of which had closer values of  $\delta$ ,  $\delta_p$  and  $\delta_h$  to those of PHBV [84]. This indicates that a similarity in the values of  $\delta_p$  and  $\delta_h$  between the polymer and the plasticizers is a factor for their effectiveness and compatibility. However, miscibility can also occur in rare cases and when least expected, such as the unique compatibility between poly(2,6-dimethyl-1,4-phenylene oxide) (PPO) and polystyrene (PS) which led to commercially significant products [127]. Blends made from PPO and PS showed complete miscibility at all compositions and previous instances of non-homogeneity were attributed to insufficient mixing [128,129].

### 6.3 Plasticizing with DHPS

Melt blending of DHPS with a-PHB resulted in blends with higher elongation at break, higher flexibility and higher tensile strength. The addition of 40 PHR DHPS to a-PHB increased its elongation from 65% to 85%, decreased its elastic modulus from 7 MPa to 3 MPa, and increased its tensile strength from 0.3 MPa to 0.4 MPa. These results are, however, considered preliminary since the experimental data of the a-PHB blend with 40 PHR is based on one tested sample only.

Similar softening effects are observed upon the melt blending of DHPS with PHBV, with blends composed of 20 wt% PHBV and 80 wt% a-PHB and already plasticized with ESO/SA, and with a-PHB already plasticized with ESO/SA, in which the addition of DHPS

resulted in blends with lower elastic modulus compared to either PHBV or blends plasticized with ESO/SA (t-test,  $p < 0.05$ ). However, these blends exhibited lower tensile strength and lower elongation at break upon the addition of DHPS (t-test,  $p < 0.05$ ). The addition of 40 PHR DHPS to PHBV decreased its elastic modulus from 270 MPa to 240 MPa, decreased its tensile strength from 21 MPa to 11 MPa, and decreased its elongation at break from 8% to 6% compared to neat PHBV. Similarly, the addition of 40 PHR DHPS to blends composed of 20 wt% PHBV and 80 wt%  $\alpha$ -PHB and already plasticized with 5 PHR ESO and 1 PHR SA decreased its elastic modulus from 43 MPa to 20 MPa, decreased its tensile strength from 0.6 MPa to 0.4 MPa, and decreased its elongation at break from 30% to 15% compared to PHBV/ $\alpha$ -PHB (20:80) plasticized with ESO/SA.

Similar effects were also observed with the addition of DHPS to blends composed of  $\alpha$ -PHB already plasticized with 5 PHR ESO and 1 PHR ESO, in which the addition of 40 PHR DHPS decreased its elastic modulus from 13 MPa to 6 MPa, decreased its tensile strength from 0.4 MPa to 0.2 MPa, and decreased its elongation at break from 92% to 57% compared to  $\alpha$ -PHB blends plasticized with ESO/SA. Additionally, it resulted in a slight reduction in  $T_g$  from  $-25\text{ }^{\circ}\text{C}$  to  $-28\text{ }^{\circ}\text{C}$  compared to  $\alpha$ -PHB blends plasticized with ESO/SA, with no effects on the heating and cooling isotherms.

Although the melt blending of DHPS had alternating effects on the tensile strength and elongation at break of  $\alpha$ -PHB compared to PHBV and blends already plasticized with ESO/SA, it resulted in a consistent increase in flexibility to all blends. Such softening effects are opposite to the slight toughening effects observed with the melt blending of ESO/SA with polymers and neat polymer blends.

To analyze the compatibility of DHPS and compare its effects on the polymers and polymer blends with those of ESO/SA, the solubility parameters of DHPS, shown in Table 6.2, are evaluated using the same method described previously. The detailed calculations are provided in Appendix A. The  $\delta$  value of DHPS is comparable to those of ESO and SA, which represents a similarity in the solubility potentials between DHPS, ESO and SA.

However, the  $\delta_p$  value of DHPS is closer to that of the polymers than ESO and SA, where  $\delta_p$  of DHPS is  $3.6 \text{ MPa}^{1/2}$  compared to  $1.9 \text{ MPa}^{1/2}$  and  $2.9 \text{ MPa}^{1/2}$  for ESO

**Table 6.2** – Solubility parameters of polymers, ESO/SA and DHPS including: overall solubility parameter ( $\delta$ ), dispersion component ( $\delta_d$ ), polar component ( $\delta_p$ ) and hydrogen bonding component ( $\delta_h$ ) of the polymers, ESO/SA and DHPS.

Repeat Unit	$\delta$	$\delta_d$	$\delta_p$	$\delta_h$
	( $\text{MPa}^{1/2}$ )	( $\text{MPa}^{1/2}$ )	( $\text{MPa}^{1/2}$ )	( $\text{MPa}^{1/2}$ )
3HV	21.9	16.8	10.5	9.4
3HB	22.2	16.4	12.3	8.4
4HB	22.6	17.0	12.3	8.4
ESO	16.1	14.9	1.9	5.9
SA	18.7	16.5	2.9	8.3
DHPS	17.4	16.1	3.7	5.5

and SA, respectively. The results of this study support the findings described previously, in which similarities in the  $\delta_p$  values between the polymers and the plasticizers can play an important factor in their effectiveness and compatibility. The negative effects of the addition of DHPS on the mechanical properties of blends containing PHBV and blends containing ESO and SA could be due to plasticizer over-dosage and phase separation. Further studies with lower DHPS dosages would provide better foundations to evaluate the plasticizer effectiveness and compatibility.

#### 6.4 Crosslinking using DCP and filling with $\text{CaCO}_3$

Melt blending of DCP and  $\text{CaCO}_3$  with blends composed of 20% wt PHBV and 80 wt% a-PHB resulted in higher tensile strength, lower flexibility and lower elongation at break (t-test,  $p < 0.05$ ), with no significant effects on either  $T_g$  or  $T_m$  (t-test,  $p > 0.05$ ). The addition of 10 PHR  $\text{CaCO}_3$  and 1 PHR DCP to PHBV/a-PHB (20:80) increased its elastic modulus from 22 MPa to 65 MPa, increased its tensile strength from 0.6 MPa to 1.4 MPa and decreased its elongation at break from 44% to 24% compared to the neat polymer blend.



Such toughening effects are expected as successful crosslinking could result in blends with higher molecular weights. Gel permeation chromatography (GPC) testing experiments would be useful in this case to evaluate the changes in molecular weights upon the addition of  $\text{CaCO}_3$ /DCP compared to neat polymers and polymer blends and develop correlations between molecular weights and thermal/mechanical properties. In a study by *Bustos et al*, the melt blending of  $\text{CaCO}_3$  and DCP with a-PHB under similar processing conditions resulted in similar toughening effects and increased the tensile strength of a-PHB, but with contrary effects on elongation at break [111]. The addition of 1 PHR of DCP to a-PHB increased its elastic modulus from 3.9 MPa to 7.5 MPa, increased its tensile strength from 0.4 MPa to 1.3 MPa, and increased its elongation at break from 70% to 160%, with no significant effects on mechanical properties upon the simultaneous addition of 5 PHR of  $\text{CaCO}_3$  to the blends [111]. These contradictory effects on elongation at break could be attributed to a combination of one or more key factors: compatibility issues, miscibility issues,  $\text{CaCO}_3$  or DCP over-dosages, processing conditions or a possible interference of PHBV with crosslinking kinetics. For example, in a study by *Fei et al*, the melt blending of 1 wt% DCP with PHBV consisting of 5 wt% HV, at a mixing speed of 10 min, a processing time of 10 min and a processing temperature of 30 rpm, was found to increase its elongation at break from 4% to 11% compared to neat PHBV, with no significant effects on either its tensile strength or its elastic modulus [130]. The melt blending of 0.5 wt% DCP under same processing conditions resulted in an elongation at break of 13% [130]. Moreover,  $\text{CaCO}_3$  is generally known to result in stiffer and more brittle blends. However, it is necessary to question the compatibility and miscibility of  $\text{CaCO}_3$  with the blends. A better understanding would be realized with individual filling and crosslinking experiments using alternating  $\text{CaCO}_3$  and DCP compositions.

The melt blending of  $\text{CaCO}_3$ /DCP with PHBV/a-PHB (20:80) had no significant effects on either  $T_g$  or  $T_m$  of neat polymer blends; however, the addition of  $\text{CaCO}_3$ /DCP was accompanied with a notable change in the crystallization mechanism. The addition of  $\text{CaCO}_3$ /DCP eliminated the crystallization peak which was observed in the cooling

isotherm of PHBV/a-PHB (20:80) at  $T_c$  of 81 °C, and resulted in blends with a completely flat crystallization isotherm and no detectable  $T_c$ . Such blocking of crystallization could be attributed to restrictions in the movement of the polymer chains, resulting from sufficient cross-linking, to an extent that the components cannot move to crystallize.

Moreover, the melt blending of  $\text{CaCO}_3$  and DCP resulted in an exothermic peak at 45°C in the second heating cycle and a small exothermic peak at 28°C in the cooling cycle, as shown in Figure 5.10. The exothermic peak at 45°C can be attributed to cold crystallization effects stimulated by the melting of unreacted DCP, which has a  $T_m$  of 39 – 41 °C. As the unreacted DCP melts, it enhances the mobility of the chain segments, enabling them to reorganize and crystallize. Since the half-life of DCP at 180 °C is 0.86 min, the melt blending should ideally continue for 5 min for complete DCP decomposition [131,132]. In this experiment, a screw speed of 100 rpm was utilized to ensure sufficient mixing of the blend. The selected screw speed and the dimensions of the screw extruder utilized in this project resulted in a melt blending time of less than 1 min. Lower screw speeds down to 30 rpm can be utilized to increase the melt blending time and increase the extent of reaction; however, this would come at the cost of providing sufficient mixing and ensuring minimal thermal degradation of the polymers. Both PHBV and a-PHB are thermally unstable polymers at 180°C and prone to thermal degradation at prolonged processing times. As the rate of crosslinking decreases due to the reduction of peroxide content, the rate of thermal degradation of the polymers increases through ‘self-catalysis’ [133]. Hence, to be able to retain a crosslinked polymer blend, it is essential to maintain a thermal degradation rate lower than crosslinking rate, which will result in remains of undecomposed DCP in the blend.

## 7. CONCLUSION AND FUTURE WORK

### 7.1 Conclusion

PHBV and c-PHB exhibited no plastic deformation and were very brittle, while a-PHB exhibited plastic deformation and higher elongation at break, but at the cost of tensile strength. DSC results were consistent with the measured mechanical properties of the polymers, in which polymers with lower  $T_g$  were generally softer. However, a-PHB polymer exhibited amorphous characteristics, in which no melting or crystallization peaks were detected in its heating/cooling isotherms.

Potential synergistic effects between a-PHB and c-PHB were observed, in which the melt blending of a-PHB with either PHBV or c-PHB generally resulted in blends with intermediate thermal and mechanical properties, except for blends with 10 – 30 wt% a-PHB in c-PHB, which had higher tensile strength (t-test,  $p < 0.05$ ), compared to c-PHB and a-PHB.

ESO/SA and DHPS were both effective in plasticizing a-PHB. Melt blending of ESO/SA with a-PHB resulted in blends with higher elongation at break (t-test,  $p < 0.05$ ) and lower flexibility (t-test,  $p = 0.09$ ), with no significant effects on either tensile strength (t-test,  $p > 0.1$ ),  $T_g$  or  $T_m$ . However, melt blending of ESO/SA with blends composed of 20 wt% PHBV and 80 wt% a-PHB resulted in blends with lower elongation at break (t-test,  $p < 0.05$ ), lower flexibility (t-test,  $p = 0.07$ ) and a modified crystallization mechanism in which the plasticized blends exhibited retarded crystallization. Preliminary results of melt blending of 40 PHR DHPS with a-PHB revealed higher elongation at break, higher flexibility and higher tensile strength compared to a-PHB.

Typical toughening effects that came at the cost of elongation at break were achieved with the addition of DCP/ $\text{CaCO}_3$ . Melt blending of DCP and  $\text{CaCO}_3$  with blends composed of 20% wt PHBV and 80 wt% a-PHB resulted in blends with higher tensile strength (t-test,  $p < 0.05$ ), lower flexibility (t-test,  $p < 0.05$ ) and lower elongation at break (t-

test,  $p < 0.05$ ), with no significant effects on either  $T_g$  or  $T_m$ . These effects were accompanied with a modified crystallization mechanism, in which the addition of  $\text{CaCO}_3/\text{DCP}$  eliminated the crystallization peak which was observed in the cooling isotherm of PHBV/a-PHB (20:80) at  $T_c$  of 81 °C, and resulted in blends with a completely flat crystallization isotherm.

In this study, consistent positive and negative effects on the mechanical and thermal properties were observed with blending of different PHA resins with each other and with selected additives.

## 7.2 Future Work

The findings reported above reveal the potential of polymer blending and the selected additives to improve the mechanical and thermal properties of PHA. Future work on optimizing the compositions and processing conditions of the blends would tune their properties and ultimately qualify PHA for a wide range of novel bioplastic applications.

More specifically, it is recommended that:

1. An experimental design study be performed with varying plasticizer compositions to evaluate their effectiveness and identify optimum dosages.
2. An experimental design study be performed with varying compositions of different PHA resins to evaluate all synergistic effects and select optimum compositions that provide maximum compatibility with plasticizers.
3. A detailed morphology characterization be performed for blends with plasticizers to evaluate and/or control the size and distribution of the dispersed phase in the polymers and evaluate any tendency for phase separation or incompatibility.
4. Crosslinking and filling experiments be executed separately and with alternating  $\text{CaCO}_3$  and DCP compositions in order to evaluate their individual effects on the blends and their optimum dosages.

5. GPC testing experiments be conducted on crosslinked blends in order to evaluate the changes in molecular weight in comparison with neat polymers and to develop correlations between molecular weight and thermal/mechanical properties.
6. A detailed theoretical study be conducted to improve our understanding of mixing phenomena in co-rotating and counter-rotating screw configurations of the twin screw extruder.

## 8. ORIGINAL CONTRIBUTIONS

PHA is a polymer that is biodegradable, biocompatible and biologically-produced using renewable resources. Compared to other biodegradable and biocompatible polymers, PHAs have a key advantage in being readily produced by microorganisms using renewable resources [6].

However, PHA faces significant challenges in its commercial application mainly due to its brittle structure, low elongation at break and narrow thermal processing window [11]. Therefore, the enhancement of the mechanical and thermal properties of selected PHA resins can create economically attractive opportunities for novel bioplastic applications.

One approach is to improve the toughness and processability of PHA by compounding it with other biodegradable polymers and additives to expand their applications, and eventually stimulate commercial interest and application-specific research [26–30]. This study aimed to examine the mechanical and thermal properties of polymer blends composed of PHBV, c-PHB, a-PHB, and selected additives.

The major contributions of this work are:

- This study represents the first attempt to use ESO, SA and the novel ‘green’ plasticizer, DHPS, to plasticize polymer blends made from different PHA resins. The results of polymer blending with the selected plasticizers and the successful plasticization of a-PHB demonstrate the possibility to plasticize PHA resins using bio-based plasticizers. Such findings can stimulate future work to better understand the parameters affecting the degree of plasticization, and ultimately lead to the use of PHA in novel bioplastic applications, in which non-toxic, biocompatible and completely biodegradable plastics are desired.

- This study represents the first attempt to study the effects of polymer blending of different PHA resins with each other. The results of polymer blending and the observed synergistic effects between a-PHB and c-PHB demonstrate the ability to control the mechanical and thermal properties of different PHA resins. Such findings can stimulate future work in selecting optimum compositions of polymer blends that provide maximum compatibility with plasticizers.

## REFERENCES

- [1] Shah, A.A., Hasan, F., Hameed, A., & Ahmed, S. (2008). Biological degradation of plastics: A comprehensive review. *Biotechnology Advances*, 26, 246–265.
- [2] Rivard, C., Moens, L., Roberts, K., Brigham, J., & Kelley, S. (1995). Starch esters as biodegradable plastics: Effects of ester group chain length and degree of substitution on anaerobic biodegradation. *Enz. Microbial Tech.*, 17, 848–852.
- [3] Geyer, R., Jambeck, J.R., & Law K. L. (2017). Production, use, and fate of all plastics ever made. *Law Sci. Adv.*, 3, 1–5.
- [4] Jambeck, J.R., Geyer, R., Wilcox, C., Siegler, T. R., Perryman, M., Andrady, A., Narayan, R., & Law, K. L. (2015). Plastic waste inputs from land into the ocean. *Science*, 347, 768–771.
- [5] Vroman, I., & Tighzert, L. (2009). Review: Biodegradable Polymers. *Materials*, 2, 307–344.
- [6] Bernard, M. (2014). Industrial Potential of Polyhydroxyalkanoate Bioplastic: A Brief Review. *University of Saskatchewan Undergraduate Research Journal*, 1(1), 1–14.
- [7] Rehm, B.H. (2003). Polyester synthases: Natural catalysts for plastics. *Biochemical Journal*, 376, 15–33.
- [8] Madison, L.L., & Huisman, G.W. (1999). Metabolic engineering of poly(3-hydroxyalkanoates): from DNA to plastic. *Microbiol. Mol. Biol.*, 63(1), 21–53.
- [9] Anil Kumar, P.K., Shamala, T.R., Kshama, L., Prakash, M.H., Joshi, G.J., Chandrashekar, A., Latha Kumari, K.S., & Divyashree, M.S. (2007). Bacterial synthesis of poly(hydroxybutyrate-co-hydroxyvalerate) using carbohydrate-rich mahua (*Madhuca* sp.) flowers. *Journal of Applied Microbiology*, 103(1), 204–209.
- [10] Mercan, N., Aslim, B., Yürsekdağ, Z.N., & Beyatlı, Y. (2002). Production of poly- $\beta$ -hydroxybutyrate (PHB) by some *Rhizobium* bacteria. *Turk. J. Biol*, 26, 215–219.
- [11] Bugnicourt, E., Cinelli, P., Lazzeri, A., & Alvarez, V. (2014). Polyhydroxyalkanoate (PHA): Review of synthesis, characteristics, processing and potential applications in packaging. *eXPRESS Polymer Letters*, 8(11), 791–808.
- [12] Grassie, N., Murray, E.J., Holmes, P.A. (1984). The thermal degradation of poly(-D)- $\beta$ -hydroxybutyric acid): Part 2 — Changes in molecular weight. *Polym. Degrad. Stab.*, 6(2), 95–103.



- [13] Spyros, A., Argyropoulos, D.S., & Marchessault, R.H. (1997). A Study of Poly(hydroxyalkanoates) by Quantitative <sup>31</sup>P NMR Spectroscopy: Molecular Weight and Chain Cleavage. *Macromolecules*, 30(2), 327–329.
- [14] de Koning, G.J.M., Scheeren, A.M.C., Lemstra, P.J., Preeters, M., & Reynears, H. (1994). Crystallization phenomena in bacterial poly[(R)-3-hydroxybutyrate]: 3. Toughening via texture changes. *Polymers*, 35(21), 4598–4605.
- [15] de Koning, G.J.M., Lemstra, P.J., Hill, D.J.T., Carswell, T.G., & O'Donnell, J.H. (1992). Ageing phenomena in bacterial poly[(R)-3-hydroxybutyrate]: 1. A study on the mobility in poly[(R)-3-hydroxybutyrate] powders by monitoring the radical decay with temperature after  $\gamma$ -radiolysis at 77 K. *Polymers*, 33(15), 3295–3297.
- [16] Foster, L.J.R., Zervas, S.J., Lenz, R.W., & Fuller, R.C. (1995). The biodegradation of poly-3-hydroxyalkanoates, PHAs, with long alkyl substituents by *Pseudomonas maculicola*. *Biodegradation*, 6(1), 67–73.
- [17] Carmen, S., Wolk, S., Lenz, R.W., & Fuller, R.C. (1994). Growth and polyester production by *Pseudomonas oleovorans* on branched octanoic acid substrates. *Macromolecules*, 27(22), 6358–6362.
- [18] Valentin, H.E., Berger, P.A., Gruys, K.J., de Andrade Rodrigues, M.F., Steinbüchel, A., Tran, M., & Asrar, J. (1999). Biosynthesis and Characterization of Poly(3-hydroxy-4-pentenoic acid). *Macromolecules*, 32(22), 7389–7395.
- [19] Saito, Y., & Doi, Y. (1994). Microbial synthesis and properties of poly(3-hydroxybutyrate-co-4-hydroxybutyrate) in *Comamonas acidovorans*. *Int. J. Biol. Macromol.*, 16(2), 99–104.
- [20] Doi, Y., Kitamura, S., & Abe, H. (1995). Microbial Synthesis and Characterization of Poly(3-hydroxybutyrate-co-3-hydroxyhexanoate). *Macromolecules*, 28(14), 4822–4828.
- [21] Chandra, R., & Rustgi, R. (1998). Biodegradable polymers. *Progr. Polym. Sci.*, 23, 1273–1335.
- [22] Szegda, D., Duangphet, S., Song, J., & Tarverdi, K. (2014). Extrusion foaming of PHBV. *Journal of Cellular Plastics*, 50(2), 145–162.
- [23] Kunasundari, B., & Sudesh, K. (2011). Isolation and recovery of microbial polyhydroxyalkanoates. *eXPRESS Polymer Letters*, 5(7), 620–634.
- [24] Lenz, R.W. (1993). Biodegradable polymers. *Adv. Polym. Sci.*, 107, 1–40.
- [25] Reddy, C.S., Ghai, R., Rashmi, & Kalia, V.C. (2003). Polyhydroxyalkanoates: An overview. *Bioresource Technology*, 87(2), 137–146.

- [26] El-Hadi, A., Schnabel, R., Straube, E., Müller, G., & Henning, S. (2002). Correlation between degree of crystallinity, morphology, glass temperature, mechanical properties and biodegradation of poly(3-hydroxyalkanoate) PHAs and their blends. *Polym. Test.*, *21*(6), 665–674.
- [27] Choi, J.S., & Park, W.H. (2003). Thermal and mechanical properties of poly(3-hydroxybutyrate-co-3-hydroxyvalerate) plasticized by biodegradable soybean oils. *Macromol. Symp.*, *197*(1), 65–76.
- [28] Liu, W.J., Yang, H.L., Wang, Z., Dong, L.S., & Liu J.J. (2002). Effect of nucleating agent on the crystallization of poly(3-hydroxybutyrate-co-3-hydroxyvalerate). *J. Appl. Polym. Sci.*, *86*(9), 2145–2152.
- [29] Yu, L., Dean, K., & Li, L. (2006). Polymer blends and composites from renewable resources. *Prog. Polym. Sci.*, *31*(6), 576–602.
- [30] Avella, M., Martuscelli, E., & Raimo, M. (2000). Review properties of blends and composites based on poly(3-hydroxybutyrate) (PHB) and poly(3-hydroxybutyrate-hydroxyvalerate) (PHBV) copolymers. *J. Mater. Sci.*, *35*(2), 523–545.
- [31] Lemoigne, M. (1926). Produits de dehydration et de polymerisation de l'acide  $\beta$ -oxobutyrique. *Bull. Soc. Chim. Biol.*, *8*, 770–782.
- [32] Williamson, D. H., & Wilkinson, J. F. (1958). The isolation and estimation of the poly-beta-hydroxybutyrate inclusions of *Bacillus* species. *Journal of General Microbiology*, *19*(1), 198–209. doi:10.1099/00221287-19-1-198
- [33] Chowdhury, A.A. (1963). Poly- $\beta$ -hydroxybuttersäure abbauende Bakterien und exoenzyme. *Archives of Microbiology*, *47*, 167–200. doi:10.1007/BF00422523
- [34] Suriyamongkol, P., Weselake, R., Narine, S., Moloney, M., & Shah, S. (2007). Biotechnological approaches for the production of polyhydroxyalkanoates in microorganisms and plants—A review. *Biotechnology Advances*, *25*(2), 148–175.
- [35] Tokiwa, Y., Calabia, B.P., Ugwu, C.U., & Aiba, S. (2009). Biodegradability of plastics. *International Journal of Molecular Sciences*, *10*(9), 3722–3742.
- [36] Snell, K.D., & Peoples, O.P. (2009). PHA Bioplastic: A value-added coproduct for biomass biorefineries. *Biofuels, Bioproducts & Biorefining*, *3*(4), 456–467.
- [37] UN–Energy. (2007). Sustainable Bioenergy: A framework for decision makers. Retrieved from <http://www.fao.org/docrep/010/a1094e/a1094e00.htm>

- [38] Forni, D., Wenk, C., & Bee, G. (1999a). Digestive utilization of novel biodegradable plastic in growing pigs. *Annales de Zootechnie*, 48, 163–171.
- [39] Forni, D., Wenk, C., & Bee, G. (1999b). Novel biodegradable plastics in sheep nutrition 1. Effects of untreated plastics on digestibility and metabolic energy and nitrogen utilization. *Journal of Animal Physiology and Animal Nutrition*, 81, 31–40. doi:10.1046/j.1439-0396.1999.811189.x
- [40] Smet, M.J., Eggink, G., Witholt, B., Kingma, K., & Wynberg, H. (1983). Characterization of intracellular inclusions formed by *Pseudomonas oleovorans* during growth on octane. *J. Bacteriol*, 154(2), 870–878. Retrieved from <http://www.ncbi.nlm.nih.gov/pmc/articles/PMC217541/>
- [41] Narayan, R. (2006). Biobased and biodegradable polymer materials: Rationale, drivers, and technology exemplars. In Khemani, K. & Scholz, C. (Eds.), *Degradable polymers and materials: Principles and practice* (pp. 282–306). Washington, DC: American Chemical Society.
- [42] Koronis, G., Silva, A., & Fontul, M. (2013). Green composites: a review of adequate materials for automotive applications. *Compos. Part B*, 44(1), 120–127.
- [43] Van de Velde, K., & Kiekens, P. (2002). Biopolymers: overview of several properties and consequences on their applications. *Polym. Test.*, 21(4), 433–442.
- [44] de Konin, G. (1995). Physical properties of bacterial poly((R)-3-hydroxyalkanoates). *Can. J. Microbiol.*, 41(1), 303–309.
- [45] Choi, W.M., Kim, T.W., Park, O.O., Chang, Y.K., & Lee, J.W. (2003). Preparation and Characterization of Poly(hydroxybutyrate-co-hydroxyvalerate)–Organoclay Nanocomposites. *Journal of Applied Polymer Science*, 90(2), 525–529.
- [46] Yu, L., Dean, K., & Li, L. (2006). Polymer blends and composites from renewable resources. *Prog. Polym. Sci.*, 31(6), 576–602.
- [47] Li, S.D., Peter, H.Y., & Cheung, M.K. (2001). Thermogravimetric analysis of poly(3-hydroxybutyrate) and poly(3-hydroxybutyrate-co-3-hydroxyvalerate). *J. Appl. Polym. Sci.* 80(12), 2237–2234.
- [48] Mohanty, A.K., Misra, M., Drzal, T.L., Selke, S.E., Harte, B.R., & Hinrichsen, G. (2005). Natural fibers, and biocomposites: an introduction. In A.K. Mohanty, M. Misra, & T.L. Drzal (Eds.), *Natural Fibers, Biopolymers and Biocomposites*. CRC Press, Taylor & Francis Group, Boca Raton, 1–36 (Chapter 1).

- [49] Avella, M., Immirzi, B., Malinconico, M., Martuscelli, E., & Volpe, M.G. (1996). Reactive blending methodologies for Biopol. *Polym. Int.*, 39(3), 191–204.
- [50] Mohanty, A.K., Misra, M., & Hinrichsen, G. (2000). Biofibres, biodegradable polymers and biocomposites: An overview. *Macromol. Mater. Eng.*, 276-277(1), 1– 24.
- [51] Hsieh, W.C., Wada, Y., Mitobe, T., Mitomo, H., Seko, N., & Tamada, M. (2009). Effect of hydrophilic and hydrophobic monomers grafting on microbial poly(3-hydroxybutyrate). *J. Tw. Inst. Chem. Eng.*, 40(4), 413–417.
- [52] Amass, W., Amass, A., & Tighe, B. (1998). A Review of biodegradable polymers: uses, current developments in the synthesis and characterization of biodegradable polyesters, blends of biodegradable polymers and recent advances in biodegradation studies. *Polym. Int.*, 47(2), 89–144.
- [53] Liu, Q.S., Zhu, M.F., Wu, W.H., & Qin, Z.Y. (2009). Reducing the formation of six-membered ring ester during thermal degradation of biodegradable PHBV to enhance its thermal stability. *Polym. Degrad. Stab.*, 94(1), 18–24.
- [54] Laycock, B., Halley, P., Pratt, S., Werker, A., & Lant, P. (2013). The chemomechanical properties of microbial polyhydroxyalkanoates. *Prog. Polym. Sci.*, 38(3-4), 536–583.
- [55] Song, C., Wang, S., Ono, S., Zhang, B., Shimasaki, C., & Inoue, M. (2003). The biodegradation of poly(3-hydroxy-butyrates-co-3-hydroxyvalerate) (PHB/V) and PHB/V–degrading microorganisms in soil. *Polym. Advan. Technol.*, 14(3-5), 184–188.
- [56] Weng, Y., Wang, Y., Wang, X., & Wang, Y. (2010). Biodegradation behavior of PHBV films in a pilot-scale composting condition. *Polym. Test.*, 29(5), 579–587.
- [57] Rajendra, K.K., & Allen R.P. (2013). Impact modification of PLA using biobased, biodegradable Mirel PHB copolymer, presented in ANTEC conference, Cincinnati, Ohio.
- [58] Fei, B., Chen, C., Chen, S., Peng, S., Zhuang, Y., & Dong, L. (2004). Crosslinking of poly[(3-hydroxybutyrate)-co-(3-hydroxyvalerate)] using dicumyl peroxide as initiator. *Polym. Int.*, 53(7), 937–943.
- [59] Qiu, Z., Ikeharab, T., & Nishia, T. (2003). Miscibility and crystallization behaviour of biodegradable blends of two aliphatic polyesters. Poly(3-hydroxybutyrate-co-hydroxyvalerate) and poly(butylene succinate) blends. *Polymer*, 44, 7519–7527.
- [60] Ma, P., Hristova-Bogaerds, D.G., Zhang, Y., & Lemstra, P.J. (2014). Enhancement in crystallization kinetics of the bacterially synthesized poly(b-hydroxybutyrate) by poly(butylene succinate). *Polym. Bull.*, 71, 907–923.

- [61] Ma, P., Hristova-Bogaerds, D.G., Lemstra, P.J., Zhang, Y., & Wang, S. (2012). Toughening of PHBV/PBS and PHB/PBS Blends via In situ Compatibilization Using Dicumyl Peroxide as a Free-Radical Grafting Initiator. *Macromol. Mater. Eng.*, 297, 402–410.
- [62] Ke, Y., Zhang, X.Y., Ramakrishna, S., He, L.M., & Wu, G. (2017). Reactive blends based on polyhydroxyalkanoates: Preparation and biomedical application. *Materials Science and Engineering-C*, 70, 1107–1119.
- [63] Lau, O., & Wong, W.S. (2000). Contamination in food from packaging material. *J. Chromatogr. A.*, 882(1-2), 255–270.
- [64] Fankhauser-Noti, A., Fiselier, K., Biedermann, S., & Grob, K. (2006). Assessment of epoxidized soy bean oil (ESBO) migrating into foods: comparison with ESBO-like epoxy fatty acids in our normal diet. *J. Food Chem. Toxicol.*, 44, 1279–1286.
- [65] Duffy, E., & Gibney, M. (2007). Use of a food-consumption database with packaging information to estimate exposure to food-packaging migrants: epoxidized soybean oil and styrene monomer. *J. Food Addit. Contam.*, 24(2), 216–225.
- [66] Pedersen, G.A., Jensen, L.K., Fankhauser, A., Biedermann, S., Petersen, J. H., & Fabech, B. (2008). Migration of epoxidized soybean oil (ESBO) and phthalates from twist closures into food and enforcement of the overall migration limit. *J. Food Addit. Contam.*, 25(4), 503–510.
- [67] Biedermann, M., Fiselier, K., & Grob, K. (2008). Testing migration from the PVC gaskets in metal closures into oily foods. *Trends Food Sci. Technol.*, 19, 145–155.
- [68] Biresaw, G., Liu, Z.S., & Erhan, S.Z. (2008). Investigation of the surface properties of polymeric soaps obtained by ring-opening polymerization of epoxidized soybean oil. *J. Appl. Polym. Sci.*, 108, 1976–1985.
- [69] Ljungberg, N., & Wesslen, B. (2003). Tributyl citrate oligomers as plasticizers for poly(lactic acid): thermo-mechanical film properties and aging. *Polymer*, 44, 7679–7688.
- [70] Carole, T.M., Pellegrino, J., & Paster, M.D. (2004). Opportunities in the industrial biobased products industry. *Appl. Biochem. Bio-technol.*, 113, 871–875.
- [71] Mohanty, A.K., Misra, M., & Drzal, L.T. (2002). Sustainable Bio-Composites from Renewable Resources: Opportunities and Challenges in the Green Materials World. *J. Polym. Environ.*, 10, 19–26.

- [72] Bueno-Ferrer, C., Garrigós, M.C., & Jiménez, A. (2010). Characterization and thermal stability of poly(vinyl chloride) plasticized with epoxidized soybean oil for food packaging. *Polymer Degradation and Stability*, 95(11), 2207–2212.
- [73] Fankhauser-Noti, A., Fiselier, K., Biedermann, S., Biedermann, M., Grob, K., Armellini, F., Rieger, K., & Skjevrak, I. (2005). Epoxidized soybean oil (ESBO) migrating from the gaskets of lids into food packed in glass jars. *Eur. Food Res. Technol.*, 221, 416–422.
- [74] Fankhauser-Noti, A., & Grob, K. (2006). Migration of plasticizers from PVC gaskets of lids for glass jars into oily food: amount of gasket material in food contact, proportion of plasticizer migrating into food and compliance testing by simulation. *Trends Food Sci. Technol.*, 17, 105–112.
- [75] Biedermann, M., Fiselier, K., Marmiroli, G., Avanzini, G., Rutschmann, E., Pfenninger, S., & Grob, K. (2008). Migration from the gaskets of lids into oily foods: first results on polyadipates. *Eur. Food Res. Technol.*, 226, 1399–1407.
- [76] Yu-Qiong, X., & Jin-Ping, Q. (2009). Mechanical and Rheological Properties of Epoxidized Soybean Oil Plasticized poly(lactic acid). *Journal of Applied Polymer Science*, 112, 3185–3191.
- [77] Wang, R., Schuman, T.P. (2013). Vegetable oil-derived epoxy monomers and polymer blends: A comparative study with review. *eXPRESS Polymer Letters*, 7(3), 272–292.
- [78] Fredriksen, O. (1969). Calcium stearate-stearic Acid as lubricants for rigid poly(vinyl chloride) (PVC). Capillary rheometer measurements and extrusion properties. *Journal of Applied Polymer Science*, 13(1), 69–80.
- [79] Ismail, A.M., & Gamal, M.A.B. (2010). Water resistance, mechanical properties, and biodegradability of poly(3-hydroxybutyrate)/starch composites. *Journal of Applied Polymer Science*, 115(5), 2813–2819.
- [80] Ljungberg, N., & Wesslen, B. (2003). Tributyl citrate oligomers as plasticizers for poly(lactic acid): Thermo-mechanical film properties and aging. *Polymer*, 44, 7679–7688.
- [81] Jacobsen S., & Fritz, H. (1999). Jacobsen, S., Fritz, H.G., 1999. Plasticizing polylactide – The effect of different plasticizers on the mechanical properties. *Polym. Eng. Sci.*, 39(7), 1303–1310.
- [82] Labrecque, L., Kumar, R., Dave, V., Gross R., & McCarthy, S. (1997). Citrate esters as plasticizers for poly(lactic acid). *J. Appl. Polym. Sci.*, 66, 1507–1513.

- [83] Ljungberg N., & Wesslen, B. (2002). Thermal and mechanical properties of plasticized poly(L-lactic acid). *J. Appl. Polym. Sci.*, 86, 1227–1234.
- [84] Choi, J.S., & Park, W.H. (2004). Effect of biodegradable plasticizers on thermal and mechanical properties of poly(3-hydroxybutyrate). *Polymer Testing*, 23(4), 455–460.
- [85] Maglio, G., Migliozi A., & Palumbo, R. (2003). Thermal properties of di- and triblock copolymers of PLLA with PEO or PCL. *Polymer*, 44, 369–375.
- [86] Maglio, G., Malinconico, M., Migliozi A., & Groeninckx, G. (2004). Immiscible poly(l-lactide)/poly( $\epsilon$ -caprolactone) blends, influence of the addition of a poly(l-lactide)-poly(oxyethylene) block copolymer on thermal behavior and morphology. *Macromol. Chem. Phys.*, 205, 946–950.
- [87] Gajria, A., Dave, V., Gross R., & McCarthy, S. (1996). Miscibility and biodegradability of blends of poly(lactic acid) and poly(vinyl acetate). *Polymer*, 37(3), 437–444.
- [88] Stuart, A., McCallum, M.M., Fan, D.M., LeCaptain, D.J., Lee, C.Y., & Mohanty, D.K. (2010). Poly(vinyl chloride) plasticized with succinate esters: synthesis and characterization. *Polym. Bull.*, 65, 589–598.
- [89] Stuart, A., LeCaptain, D.J., Lee, C.Y., & Mohanty, D.K. (2013). Poly(vinyl chloride) plasticized with mixtures of succinate di-esters – synthesis and characterization. *European Polymer Journal*, 49(9), 2785–2791.
- [90] Enthropel, H.C., Dodd, P., Leask, R.L., Maric, M., & Cooper, D.G. (2013). Designing green plasticizers: Influence of alkyl chain length on biodegradation and plasticization properties of succinate based plasticizers. *Chemosphere*, 91(3), 358–365.
- [91] Elsiwi, B. (2017). Diheptyl succinate (DHPS) as a renewably-sourced green plasticizer. (Unpublished master's thesis). McGill University, Montreal, QC.
- [92] Verhoogt, H., Ramsay, B.A., and Favis, B.D. (1994). Polymer blends containing poly(3-hydroxyalkanoates) (PHAs). *Polymer*, 35(24), 5155–5169.
- [93] Xanthos, M. (2005). Polymers and Polymer Composites. In M. Xanthos (Ed.), *Functional Fillers for Plastics*. Germany: Wiley-VCH Verlag GmbH & Co. KGaA, 1–16.
- [94] Wan, C.Y., Qiao, X.Y., Zhang, Y., & Zhang, Y.X. (2003). Effect of different clay treatment on morphology and mechanical properties of PVC-clay nanocomposites. *Polymer Testing*, 22(4), 453–461.
- [95] Reynaud, E., Jouen, T., Gaunthier, C., Vigier, G., & Varlet, J. (2001). Nanofiller in polymeric matrix: a study on silica reinforced PA6. *Polymer*, 42, 8759–8768.

- [96] Cao, Y.M., Sun, J., & Yu, D.H. (2002). Preparation and properties of nano- $\text{Al}_2\text{O}_3$  particles/polyester/epoxy resin ternary composites. *Journal of Applied Polymer Science*, 83(1), 70–77.
- [97] Chan, C.M., Wu, J.S., Li, J.X., & Cheung, Y.T. (2002). Polypropylene/calcium carbonate nanocomposites. *Polymer*, 43(10), 2981–2992.
- [98] Di Lorenzo, M.L., Errico, M.E., & Avella, M. (2002). Thermal and morphological characterization of poly(ethylene terephthalate)/calcium carbonate nanocomposites. *Journal of Materials Science*, 37(11), 2351–2358.
- [99] Avella, M., Errico, M.E., & Martuscelli, E. (2001). Novel PMMA/ $\text{CaCO}_3$  nanocomposites abrasion resistant prepared by an in situ polymerization process. *Nano Letters*, 1(4), 213–217.
- [100] Solomon, D.H., & Hawthorne, D.G. (1983). *Chemistry of Pigments and Fillers*. New York: Wiley.
- [101] Papirer, E., Schultz, J., & Turchi, C. (1984). Surface properties of a calcium carbonate filler treated with stearic acid. *European Polymer Journal*, 20(12), 1155–1158.
- [102] Suito, E., Arakawa, M., & Arakawa, T. (1975). Surface Area Measurement of Powders by Adsorption in Liquid Phase. (II): Effect of Adsorbates and Solvents. *Bulletin of the Institute of Chemical Research*, Kyoto University, 33(1), 8–13.
- [103] Ding, Y., He, J., Yang, Y., Cui, S., & Xu, K. (2011). Mechanical properties, thermal stability, and crystallization kinetics of poly(3-hydroxybutyrate-co-4-hydroxybutyrate)/calcium carbonate composites. *Polymer Composites*, 32(7), 1134–1142.
- [104] Othman, M., Hashim, M.Y., Azowa, I.N., Khalid, K., & Mohamad, S.A. (2015). Effect of clamshells filler loading on the tensile properties of polyhydroxybutyrate. *Advanced Materials Research*, 115, 262–265.
- [105] Ke, Y., Zhang, X.Y., Ramakrishna, S., He, L.M., & Wu, G. (2017). Reactive blends based on polyhydroxyalkanoates: Preparation and biomedical application. *Materials Science and Engineering: C*, 70(2), 1107–1119.
- [106] Wang, R., Wang, S., Zhang, Y., Wan, C., & Ma, C. (2009). Toughening Modification of PLLA/PBS Blends via In Situ Compatibilization. *Polym. Eng. Sci.*, 49(1), 26–33.
- [107] CITI. (1992). Acute toxicity, biodegradability and bioaccumulation data (MITI): 2,4-TDA and 4,4-MDA. In *Data of Existing Chemicals Based on the CSCL Japan*, Chemicals



- Inspection and Testing Institute. Ministry of International Trade and Industry, Japan (ISBN 4-89074-101-1).
- [108] Jeong, S.B., Yang, Y.C., Chae, Y.B., & Kim, B.G. (2009). Characteristics of the treated ground calcium carbonate powder with stearic acid using the dry process coating system. *Materials Transactions*, 50(2), 409–414.
- [109] ASTM D3418-15. (2015). Standard Test Method for Transition Temperatures and Enthalpies of Fusion and Crystallization of Polymers by Differential Scanning Calorimetry, American Society for Testing and Materials, Philadelphia, Pennsylvania.
- [110] Ding, Y., He, J., Yang, Y., Cui, S., & Xu, K. (2011). Mechanical properties, thermal stability, and crystallization kinetics of poly(3-hydroxybutyrate-co-4-hydroxybutyrate)/calcium carbonate composites. *Polymer Composites*, 32(7), 1134–1142.
- [111] Bustos, M. (2017). Effect of selected additives on the mechanical and rheological properties of an amorphous poly(hydroxyalkanoate). (Unpublished master's thesis). McGill University, Montreal, QC.
- [112] ASTM D638-03. (2003). *Standard Test Method for Tensile Properties of Plastics*, American Society for Testing and Materials, Philadelphia, Pennsylvania.
- [113] Carrasco, F., Dionisi, D., Martinelli, A., & Majone, M. (2006). Thermal stability of polyhydroxyalkanoates. *J. Appl. Polym. Sci.*, 100(3), 2111–2121.
- [114] Nanda, M.R., Misra, M., & Mohanty, A.K. (2011). The effect of process engineering on the performance of PLA and PHBV blends. *Macromol. Mater. Eng.*, 296(8), 719–728.
- [115] McNeill, I., & Leiper, H. (1985). Degradation studies of some polyesters and polycarbonates. 2. Polylactide: degradation under isothermal conditions, thermal degradation mechanism and photolysis of the polymer. *Polym. Degrad. Stab.*, 11(4), 309–326.
- [116] Holmes, P.A. (1988). Biologically produced (R)-3-hydroxyalkanoate polymers and copolymers. In *Development in crystalline polymers. Vol. 2*. Edited by D.C. Bassett. Elsevier, London, 1–65.
- [117] Panaitescu, D.M., Nicolae, C.A., Frone, A.N., Chiulan, I., Stanescu, P.O., Draghici, C., Iorga, M., & Mihailescu, M. (2017). Plasticized poly(3-hydroxybutyrate) with improved melt processing and balanced properties. *Journal of Applied Polymer Science*, 134(19), 1–14.

- [118] Barham, P. J., Keller, A., Otun, E.L., & Holmes, P.A. (1984). Crystallization and morphology of a bacterial thermoplastic: poly-3-hydroxybutyrate. *Journal of Materials Science*, 19(9), 2781–2784.
- [119] Qiua, Z., Ikeharab, T., & Nishia, T. (2003). For cold crystallization - Miscibility and crystallization behaviour of biodegradable blends of two aliphatic polyesters. Poly(3-hydroxybutyrate-co-hydroxyvalerate) and poly(butylene succinate) blends. *Polymer*, 44, 7519–7527.
- [120] Wellen, R.M.R., Rabello, M.S., Júnior, I.C.A., Fachine, G.J.M., & Canedo, E.L. (2015). Melting and crystallization of poly(3-hydroxybutyrate): effect of heating/cooling rates on phase transformation. *Polímeros*, 25(3), 296–304.
- [121] Wellen, R.M.R., & Rabello, M.S. (2005). The kinetics of isothermal crystallization and tensile properties of poly(ethylene) terephthalate. *Journal of Materials Science*, 40(23), 6099–6104.
- [122] Ziaee, Z., & Supaphol, P. (2006). Non-isothermal melt- and cold-crystallization kinetics of poly(3-hydroxybutyrate). *Polymer Testing*, 25(6), 807–818.
- [123] Wellen, R.M.R., & Rabello, M.S. (2009). Antinucleating action of polystyrene on the isothermal cold crystallization of poly(ethylene terephthalate). *Journal of Applied Polymer Science*, 114(3), 1884–1895.
- [124] Requena, R., Jiménez, A., Vargas, M., & Chiralt, A. (2016). Effect of plasticizers on thermal and physical properties of compression-moulded poly[(3-hydroxybutyrate)-co- (3-hydroxyvalerate)] films. *Polymer Testing*, 56, 45–53.
- [125] Van Krevelen, D.W., & Te Nijenhuis, K. (2009). Chapter 7 - Cohesive Properties and Solubility, In *Properties of Polymers (Fourth Edition)*, Elsevier, Amsterdam, 2009, 189–227.
- [126] Labrecque, L.V., Dave, V., Gross, R.A., & McCarthy, S.P. (1995). ANTEC '95, 1819–1823.
- [127] MacKnight, W.J., Karasz, F.E., & Fried, J.R. (1978). Chapter 5: Solid state transition behavior of blends. In D.R. Paul and S. Newman (Eds.), *Polymer Blends (Vol. 1)*. New York: Academic Press, 185–242.
- [128] Shultz, A.R., & Beach, M. (1974). Thermo-optical, differential calorimetric, and dynamic viscoelastic transitions in poly(2,6-dimethyl-1,4-phenylene oxide) (PPO resin) blends with poly-p-chlorostyrene and with styrene-p-chlorostyrene statistical copolymers. *Macromolecules*, 7(6), 902–909.

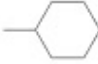
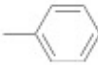
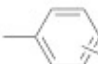
- [129] Shultz, A.R., & Gendron, M. (1972). Thermo-optical and differential scanning calorimetric observations of mobility transitions in polystyrene-poly(2,6-dimethyl-1,4-phenylene oxide) blends. *Journal of Applied Polymer Science*, 16(2), 461–471.
- [130] Fei, B., Chen, C., Chen, S., Peng, S., Zhuang, Y., An, Y., & Dong, L. (2004). Crosslinking of poly[(3-hydroxybutyrate)-co-(3-hydroxyvalerate)] using dicumyl peroxide as initiator. *Polymer International*, 53(7), 937–943.
- [131] Bodley, M.W. (2017). Functional nitroxyls in polypropylene based thermoplastic vulcanizates. (Master's thesis, Queen's University). Retrieved from [https://qspace.library.queensu.ca/bitstream/handle/1974/15863/Bodley\\_Michael\\_W\\_201705\\_M.A.Sc.pdf?sequence=2](https://qspace.library.queensu.ca/bitstream/handle/1974/15863/Bodley_Michael_W_201705_M.A.Sc.pdf?sequence=2)
- [132] Chatterjee, T., Wiessner, S., Naskar, K., & Heinrich, G. (2014). Novel thermoplastic vulcanizates (TPVs) based on silicone rubber and polyamide exploring peroxide cross-linking. *eXPRESS Polymer Letters*, 8(4), 220–231.
- [133] Chen, C., Fei, B., Peng, S., Zhuang, Y., & Dong, L. (2002). The kinetics of the thermal decomposition of poly(3-hydroxybutyrate) and maleated poly(3-hydroxybutyrate). *J. Appl. Polym. Sci.*, 84(9), 1789–1796.
- [134] Noda, I., Marchessault, R.H., & Terada, M. (2009). Poly(hydroxybutyrate). In J. E. Mark (Ed.), *Polymer Data Handbook (edition 2)*. New York: Oxford University Press, 741–752.
- [135] MSDS rac-3-hydroxypentanoic acid (2017). Safety Data Sheet. Santa Cruz Biotechnology Inc., 1, 1–6. Retrieved from: <http://datasheets.scbt.com/sds/aghs/en/sc-488462.pdf>
- [136] Govedarica, O., Janković, M., Sinadinović-Fišer, S., Radičević, R., Erceg, T., Vukić, N., & Budinski-Simendić, J. (2016). Densities of soybean oil, epoxidized soybean oil and acetic acid binary mixtures: experimental data and correlation. Paper published in the proceedings of the Physical Chemistry 2016 conference, Belgrade, 681–684.
- [137] MSDS epoxidized soybean oil (2014). GPS Safety Summary. Arkema, 1–4. Retrieved from: <https://www.arkema.com/export/shared/.content/media/downloads/socialresponsability/safety-summaries/Functional-Additives-ESBO-VIKOFLEX-7170-GPS-2014-11-30-V0.pdf>
- [138] NICNAS STD/1508 Public Report (2014). Butanedioic acid, 1,4-diheptyl ester (INCI name: Diheptyl succinate). National Industrial Chemicals Notification and Assessment Scheme, 1–17.

## APPENDIX – A

### Calculation of Solubility Parameters

The solubility parameters were calculated based on the solubility parameter component group contributions method by Hoftyzer–Van Krevelen [125]. The solubility parameter component group contributions, shown in Table A, considers similarities in some chemical and physical properties of chemical compounds when found in different molecules. First, each molecule of interest was analyzed and weighed with respect to the various chemical compounds forming the molecule. Then, component group contributions were utilized to calculate the overall solubility parameter ( $\delta$ ), dispersion component ( $\delta_d$ ), polar component ( $\delta_p$ ) and hydrogen bonding component ( $\delta_h$ ). The calculation tables for the solubility parameters of the molecules of interest are shown in Tables A2 – A7.

**Table A1** – Solubility parameter component group contributions (Hoftyzer–Van Krevelen Method) [125].

Structural group	$F_{di}$ (MJ/m <sup>3</sup> ) <sup>1/2</sup> • mol <sup>-1</sup>	$F_{pi}$ (MJ/m <sup>3</sup> ) <sup>1/2</sup> • mol <sup>-1</sup>	$E_{hi}$ J/mol
-CH <sub>3</sub>	420	0	0
-CH <sub>2</sub> -	270	0	0
>CH-	80	0	0
>C<	-70	0	0
=CH <sub>2</sub>	400	0	0
=CH-	200	0	0
=C<	70	0	0
	1620	0	0
	1430	110	0
 (o, m, p)	1270	110	0
-F	(220)	-	-
-Cl	450	550	400
-Br	(550)	-	-
-CN	430	1100	2500
-OH	210	500	20,000
-O-	100	400	3000
-COH	470	800	4500
-CO-	290	770	2000
-COOH	530	420	10,000
-COO-	390	490	7000
HCOO-	530	-	-
-NH <sub>2</sub>	280	-	8400
-NH-	160	210	3100
>N-	20	800	5000
-NO <sub>2</sub>	500	1070	1500
-S-	440	-	-
=PO <sub>4</sub>	740	1890	13,000
Ring	190	-	-
One plane of symmetry	-	0.50×	-
Two planes of symmetry	-	0.25×	-
More planes of symmetry	-	0×	0×

Molecular structures of components:

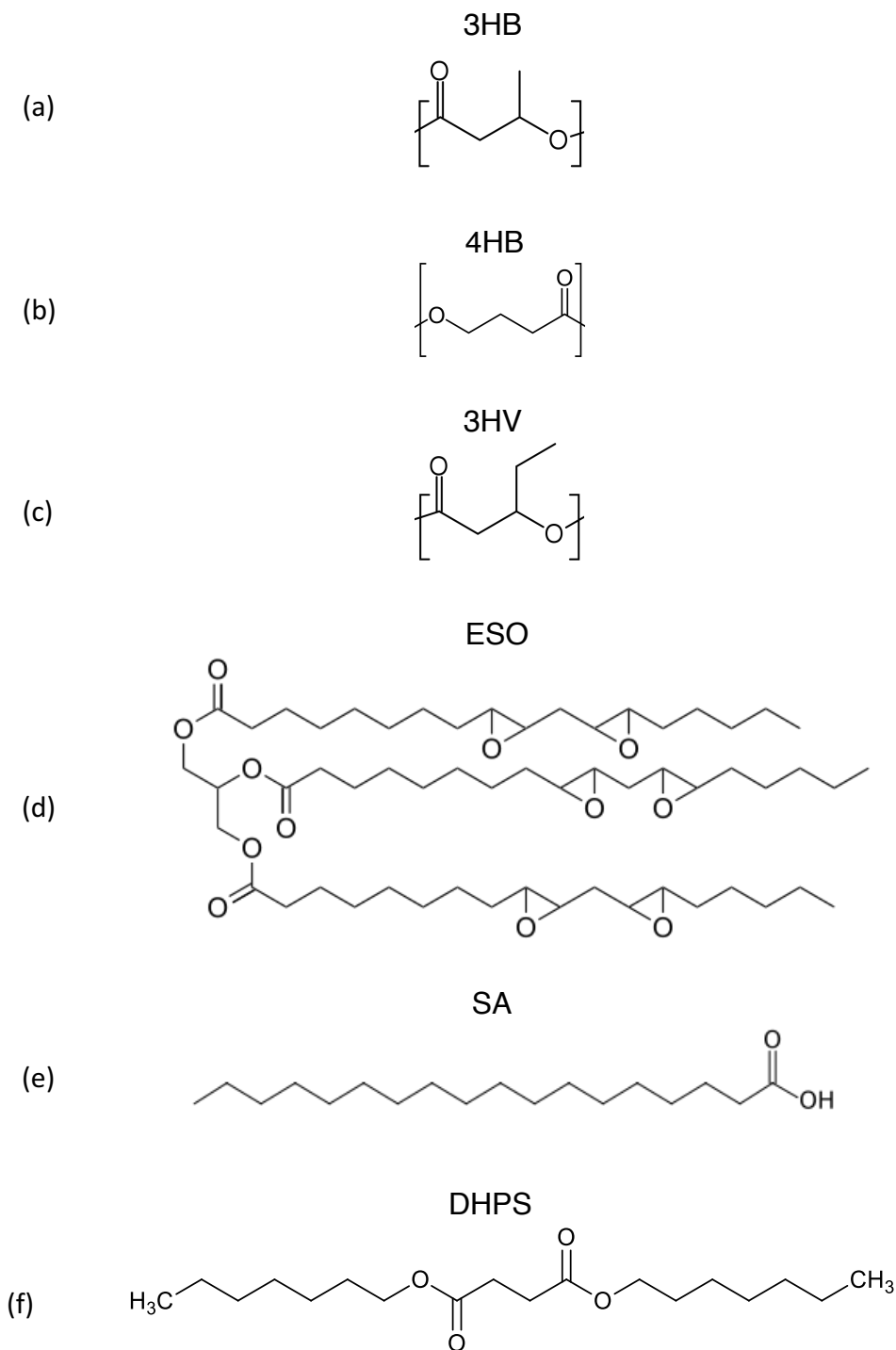


**Figure A1** – Molecular structures of: (a) 3HB; (b) 4HB; (c) 3HV; (d) ESO; (e) SA; (f) DHPS.

Formulas used to calculate the overall solubility parameter and solubility components (Hoftyzer and Van Krevelen method) [125]:

$$\delta_d = \frac{\sum F_{di}}{V} \quad (\text{Eq. A1})$$

$$\delta_p = \frac{\sqrt{\sum F_{pi}^2}}{V} \quad (\text{Eq. A2})$$

$$\delta_h = \frac{\sum F_{hi}}{V} \quad (\text{Eq. A3})$$

$$\delta^2 = \delta_d^2 + \delta_p^2 + \delta_h^2 \quad (\text{Eq. A4})$$

Calculation Tables:

**Table A2** – Calculation table for solubility parameters of 3HB.

3-hydroxybutyrate (3HB)							
	n	F <sub>di</sub>	F <sub>pi</sub> <sup>2</sup>	E <sub>hi</sub>	n*F <sub>di</sub>	n*F <sub>pi</sub> <sup>2</sup>	n*E <sub>hi</sub>
CH <sub>2</sub>	1	270	0	0	270	0	0
CO	1	290	592900	2000	290	592900	2000
O	1	100	160000	3000	100	160000	3000
CH	1	80	0	0	80	0	0
CH <sub>3</sub>	1	420	0	0	420	0	0
SUM					1160	752900	5000

MW	86.09		g/mol	[134]
ρ	1.177	1.262	g/cm <sup>3</sup>	[134]
V	73.14	68.22	cm <sup>3</sup> /mol	

	MIN	MAX	Mean
δ <sub>d</sub>	15.86	17.00	<b>16.4</b>
δ <sub>p</sub>	11.86	12.72	<b>12.3</b>
δ <sub>h</sub>	8.27	8.56	<b>8.4</b>
δ	21.46	22.90	<b>22.2</b>

**Table A3** – Calculation table for solubility parameters of 4HB.

4-hydroxybutyrate (4HB)							
	n	F <sub>di</sub>	F <sub>pi</sub> <sup>2</sup>	E <sub>hi</sub>	n*F <sub>di</sub>	n*F <sub>pi</sub> <sup>2</sup>	n*E <sub>hi</sub>
CH <sub>2</sub>	3	270	0	0	810	0	0
CO	1	290	592900	2000	290	592900	2000
O	1	100	160000	3000	100	160000	3000
CH	0	80	0	0	0	0	0
CH <sub>3</sub>	0	420	0	0	0	0	0
SUM					1200	752900	5000

MW	86.09		g/mol	[134]
ρ	1.177	1.262	g/cm <sup>3</sup>	[134]
V	73.14	68.22	cm <sup>3</sup> /mol	

	MIN	MAX	<u>Mean</u>
δ <sub>d</sub>	16.41	17.59	<b>17.0</b>
δ <sub>p</sub>	11.86	12.72	<b>12.3</b>
δ <sub>h</sub>	8.27	8.56	<b>8.4</b>
δ	21.87	23.34	<b>22.6</b>



**Table A4** – Calculation table for solubility parameters of 3HV.

3-hydroxyvalerate (3HV)							
	n	F <sub>di</sub>	F <sub>pi</sub> <sup>2</sup>	E <sub>hi</sub>	n*F <sub>di</sub>	n*F <sub>pi</sub> <sup>2</sup>	n*E <sub>hi</sub>
CH <sub>2</sub>	2	270	0	0	540	0	0
CO	1	290	592900	2000	290	592900	2000
O	2	100	160000	3000	200	320000	6000
CH	1	80	0	0	80	0	0
CH <sub>3</sub>	1	420	0	0	420	0	0
SUM					1530	912900	8000

MW	100.13		g/mol	[135]
ρ	1.0	1.2	g/cm <sup>3</sup>	[135]
V	100.13	83.44	cm <sup>3</sup> /mol	

	MIN	MAX	<u>Mean</u>
δ <sub>d</sub>	15.28	18.34	<b>16.8</b>
δ <sub>p</sub>	9.54	11.45	<b>10.5</b>
δ <sub>h</sub>	8.94	9.79	<b>9.4</b>
δ	20.11	23.73	<b>21.9</b>

**Table A5** – Calculation table for solubility parameters of ESO.

epoxidized soybean oil (ESO)							
	n	F <sub>di</sub>	F <sub>pi</sub> <sup>2</sup>	E <sub>hi</sub>	n*F <sub>di</sub>	n*F <sub>pi</sub> <sup>2</sup>	n*E <sub>hi</sub>
CH <sub>2</sub>	38	270	0	0	10260	0	0
CO	3	290	592900	2000	870	1778700	6000
O	9	100	160000	3000	900	1440000	27000
CH	13	80	0	0	1040	0	0
CH <sub>3</sub>	3	420	0	0	1260	0	0
OH	0	210	250000	20000	0	0	0
SUM					14330	3218700	33000

MW	963		g/mol	[136]
ρ	0.994	1.01	g/cm <sup>3</sup>	[137]
V	968.81	953.47	cm <sup>3</sup> /mol	

	MIN	MAX	<u>Mean</u>
δ <sub>d</sub>	14.79	15.03	<b>14.9</b>
δ <sub>p</sub>	1.85	1.88	<b>1.9</b>
δ <sub>h</sub>	5.84	5.88	<b>5.9</b>
δ	16.01	16.25	<b>16.1</b>

**Table A6** – Calculation table for solubility parameters of SA.

stearic acid (SA)							
	n	F <sub>di</sub>	F <sub>pi</sub> <sup>2</sup>	E <sub>hi</sub>	n*F <sub>di</sub>	n*F <sub>pi</sub> <sup>2</sup>	n*E <sub>hi</sub>
CH <sub>2</sub>	16	270	0	0	4320	0	0
CO	1	290	592900	2000	290	592900	2000
O	0	100	160000	3000	0	0	0
CH	0	80	0	0	0	0	0
CH <sub>3</sub>	1	420	0	0	420	0	0
OH	1	210	250000	20000	210	250000	20000
SUM					5240	842900	22000

MW	284.484		g/mol	[137]
ρ	0.847	0.9408	g/cm <sup>3</sup>	[137]
V	335.87	302.39	cm <sup>3</sup> /mol	

	MIN	MAX	<u>Mean</u>
δ <sub>d</sub> =	15.60	17.33	<b>16.5</b>
δ <sub>p</sub> =	2.73	3.04	<b>2.9</b>
δ <sub>h</sub> =	8.09	8.53	<b>8.3</b>
δ =	17.79	19.55	<b>18.7</b>

**Table A7** – Calculation table for solubility parameters of DHPS.

diheptyl succinate (DHPS)							
	n	F <sub>di</sub>	F <sub>pi</sub> <sup>2</sup>	E <sub>hi</sub>	n*F <sub>di</sub>	n*F <sub>pi</sub> <sup>2</sup>	n*E <sub>hi</sub>
CH <sub>2</sub>	14	270	0	0	3780	0	0
CO	2	290	592900	2000	580	1185800	4000
O	2	100	160000	3000	200	320000	6000
CH	0	80	0	0	0	0	0
CH <sub>3</sub>	2	420	0	0	840	0	0
OH	0	210	250000	20000	0	0	0
SUM					5400	1505800	10000

MW	314.466		g/mol	[138]
ρ	0.929	0.945	g/cm <sup>3</sup>	[138]
V	338.50	332.77	cm <sup>3</sup> /mol	

	MIN	MAX	<u>Mean</u>
δ <sub>d</sub> =	15.95	16.23	<b>16.1</b>
δ <sub>p</sub> =	3.63	3.69	<b>3.7</b>
δ <sub>h</sub> =	5.44	5.48	<b>5.5</b>
δ =	17.24	17.52	<b>17.4</b>